2005

An Investigation of Rupture in Thin Fluid Films

Robin Baur
Harvey Mudd College

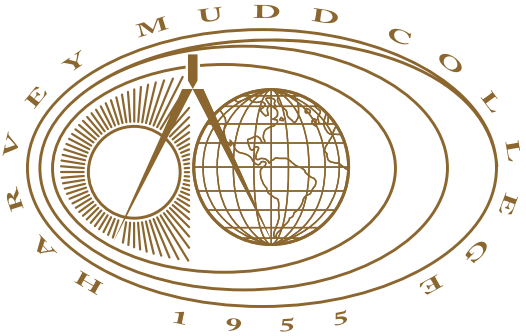

An Investigation of Rupture in Thin Fluid Films

Robin M. Baur

Professor Andrew J. Bernoff, Advisor

Professor Jon Jacobsen, Reader

December, 2005

HARVEY MUDD
COLLEGE

Department of Mathematics

Abstract

The behavior of a fluid with a thin capillary meniscus can be modelled on a one-dimensional domain $\Omega = [-L, L]$ by the thin film equation

$$h_t = -(h^n h_{xxx})_x$$

with boundary conditions $h_x(\pm L) = \pm\alpha$ (giving a fixed contact angle) and $h_{xxx}(\pm L) = 0$ (prohibiting mass flux).

It is desirable to know whether or not such a film experiences *rupture*; that is, whether there exists some x_0, t_0 (with t_0 possibly ∞) such that $h(x_0, t_0) = 0$, corresponding to the appearance of a dry spot. We approach this problem using energy methods, which use the conservation or dissipation of quantities such as mass, surface area, coating energy, and other more abstract quantities to describe the behavior of the fluid.

We present a brief analysis of the behavior of some of these energies, as well as a proof that, given certain assumptions, rupture cannot occur in a thin capillary meniscus for $n > 4$ and, in more restricted cases, for $n > 7/2$. We also show that rupture must occur for $0 < n < 1/2$. We describe the asymptotic behavior of the regions in which rupture occurs.

We also describe the numerical implementation of this problem and the advantages and drawbacks of using certain prewritten solvers in MATLAB and new implementations of θ-weighted schemes and the Newton-Raphson method. We propose uses of these numerical methods to make further progress on the problem.

Contents

Abstract **iii**

Acknowledgments **ix**

1 Introduction **1**
1.1 Preliminaries 1
1.2 The Problems 7
1.3 Prior Research 8
1.4 A Prior No-Rupture Proof 10

2 Theory **13**
2.1 Our Model 13
2.2 Energies 15
2.3 Minimizers 18
2.4 Boundedness 21
2.5 No Rupture 22
2.6 Refinement of Rupture Bounds 25
2.7 Rupture 27
2.8 Asymptotics 30

3 Numerical Analysis **33**
3.1 Implementation 33
3.2 Observation of Film Behavior 39
3.3 Refinement Analysis 43

4 Future Work **47**
4.1 General Open Problems 47
4.2 Problems Specific to the Capillary Meniscus 48

Bibliography **51**

List of Figures

1.1 A thin film on a solid substrate. 2

2.1 Solid, liquid, and vapor interfaces at the contact line. 14
2.2 Examples of films with positive and negative contact angle. 15
2.3 A representative plot of h_{xx}. 28

3.1 A ruptured film with $n = 1$ and $t = .00675$. 40
3.2 A small droplet forming in a film for $n = 2$, $t = .15$. 40
3.3 A close-up of the rupture in Fig. 3.1 for $n = 1$, $t = .00675$. . . 41
3.4 A close-up of a squeeze point in Fig. 3.2 for $n = 2$, $t = .15$. . 41
3.5 Convergence to a minimizer for $n = 2$, $t = .05$. 42
3.6 Minimum thickness of the film over time. 43
3.7 Refinement analysis plot for `ode15s` solver. 44

Acknowledgments

First thanks are due of course to my advisor, Andrew Bernoff, without whose guidance this project would never have gotten off the ground, and to my reader, Jon Jacobsen, for his sharp eyes and insights.

During the summer of 2005, this research was graciously hosted by the UCLA Applied Mathematics Lab under the direction of Professor Andrea Bertozzi, whose comments on this problem were indispensable.

In addition, this research has been supported by a Beckman Research Grant.

Thanks also to Benj Azose and Lori Thomas for their support, and apologies for a request I unfortunately had to leave unfilled. To all participants in the ICT, my admiration and gratitude.

Finally, for seemingly infinite patience throughout this entire process, Eli Bogart has my warmest thanks and love.

Chapter 1

Introduction

1.1 Preliminaries

1.1.1 The Thin Film Equation

When sheets of fluid are thin enough, their behavior is primarily driven by their surface tension rather than by bulk matter transport (convection), gravity, or molecular interactions such as van der Waals forces. This behavior can then be modelled by a fourth-order nonlinear degenerate diffusion equation, namely

$$h_t = -\nabla \cdot (f(h)\nabla \Delta h) \tag{1.1}$$

with $f(h) \sim h^n$ as $h \to 0$, which in the one-dimensional case with $f(h)$ exactly equal to h^n becomes

$$h_t = -(h^n h_{xxx})_x, \tag{1.2}$$

which is known as the *thin film equation* or the *lubrication equation*.

Different values of the exponent n correspond to different physical conditions. For instance, $n = 3$ corresponds to free motion of a fluid laid atop a solid substrate, and $n = 1$ corresponds to fluid forming a thin neck in a Hele-Shaw cell, that is, a fluid constrained to the space between two plates, where the plate separation is much larger than the width of the fluid, as described in Almgren (1996), Almgren et al. (1996), Constantin et al. (1993), and Dupont et al. (1993).

Note that if a film $h(x,t)$ is to be considered thin, it must not only be primarily driven by surface tension, but must also satisfy the small-slope requirement, $|h_x(x,t)| \ll 1$. We will use this fact frequently in theoretical

arguments, but numerically generated figures have been rescaled so that any interesting behavior is visible, and therefore may not seem to obey this requirement.

Physical Derivation

The derivation of the thin film equation is involved, but it is possible to trace the more significant points without losing the sense of the matter. Here we will only consider the derivation of the equation for $n = 3$, the case of a fluid moving freely on a solid substrate. There is a more detailed derivation including terms that account for gravity and long-range intermolecular forces in Myers (1998).

We begin by considering a layer of fluid on a solid substrate as in Fig. 1.1, where x is the horizontal spatial coordinate, y is the vertical spatial coordinate, and $h(x)$ is the height of the top of the layer of fluid immediately above point x. We will denote the velocity of the fluid by $\vec{u}(x,y) = (u(x,y), v(x,y))$. This notation, while potentially confusing, is unfortunately conventional; for the sake of clarity, we will always use the vector bar when referring to the full vector velocity $\vec{u}$.

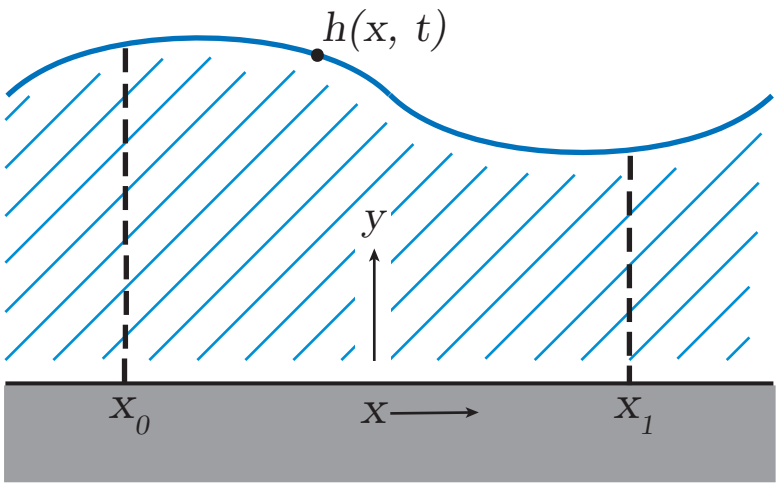

Figure 1.1: A thin film on a solid substrate.

Consider two points x_0 and x_1. Supposing that mass is conserved, we can set the flux into and out of the region at x_0 and x_1 to be equal, which

allows us to derive the *kinematic condition*,

$$h_t + \frac{\partial}{\partial x} \int_0^h u(x,y)\, dy = 0. \tag{1.3}$$

If we assume that the fluid is incompressible, we can also state that

$$\nabla \cdot \vec{u} = 0. \tag{1.4}$$

We also require a *no-slip* condition, in which the velocity of the film at the layer of contact with the solid substrate is specified to be 0, i.e.,

$$\vec{u}(x,0) = \vec{0} \tag{1.5}$$

We make use of the Navier-Stokes equation for fluids, given by

$$\rho[\vec{u}_t + (\vec{u} \cdot \nabla)\vec{u}] = \vec{F} - \nabla P + \mu \Delta \vec{u}, \tag{1.6}$$

which, while complicated, arises from a momentum balance requirement. The right-hand side contains the body force $\vec{F}$, the pressure in the body ∇P, and the Stokes drag $\mu \Delta \vec{u}$.

Finally, if we define a stress tensor T_{ij} accounting for the pressure and the Stokes drag, we also claim that the forces due to this stress tensor must be balanced by the forces due to external atmospheric pressure on the boundary of the region and by the forces due to the surface tension. If we define P_0 to be the external pressure, κ to be the curvature, and γ to be the surface tension, we can then write

$$T_{ij}\hat{n}_j = -(P_0 - \gamma\kappa)\hat{n}_i \tag{1.7}$$

(making use of the standard Einstein summation convention on the left-hand side), where $\hat{n}_i$ is the unit outward normal in the ith coordinate.

We then introduce a set of new variables: the length scale L, the typical velocity U, the tension $\mathcal{T}$, and the kinematic viscosity $\nu = \mu/\rho$. The Reynolds number $\mathrm{Re} = UL/\nu$ is also a measure of the viscosity of the film; low Reynolds number corresponds to high kinematic viscosity. Also specify that $\vec{F} = \vec{0}$, meaning there are no body forces on this fluid (the effects of gravity, for instance, are negligible). Then we can write $x = Lx'$, $y = Ly'$, and $h = Lh'$ to nondimensionalize the spatial variables, and similarly write $\vec{u} = U\vec{u}'$, $P - P_0 = \rho U^2 P'$, $\kappa = \kappa'/L$, and $t = (L/U) \cdot t'$ to nondimensionalize all other quantities. The first three equations above are left unchanged

by this nondimensionalization; once we drop the primes from the new variables, Eqn. 1.6 and Eqn. 1.7 can be rewritten as

$$[\vec{u}_t + (\vec{u} \cdot \nabla)\vec{u}] = \frac{1}{\mathrm{Re}}\Delta\vec{u} - \nabla P \tag{1.8}$$

and

$$\frac{1}{\mathrm{Re}}\left[\frac{\partial \vec{u}_i}{\partial x_j} + \frac{\partial \vec{u}_j}{\partial x_i}\right] \cdot \hat{n}_j = P\hat{n}_i + \frac{\mathcal{T}}{\rho U^2 L}\kappa\hat{n}_i. \tag{1.9}$$

Specify a new pressure $\tilde{P} = P \cdot \mathrm{Re}$ so that we can rewrite Eqn. 1.8 yet again as

$$[\vec{u}_t + (\vec{u} \cdot \nabla)\vec{u}] \cdot \mathrm{Re} = \Delta\vec{u} - \nabla\tilde{P}. \tag{1.10}$$

We wish to consider films with very high viscosity, so that $\mathrm{Re} \to 0$. A relaxation of this assumption in the derivation of the lubrication equation is discussed in Myers (1998). Then the left side of this equation becomes insignificant and we are left simply with

$$\Delta\vec{u} = \nabla\tilde{P}. \tag{1.11}$$

If we also note that $\frac{\mathrm{Re}}{\rho UL} = \mu$, we can rewrite $\frac{\mathcal{T}\mathrm{Re}}{\rho U^2 L}$ as $\frac{\mathcal{T}}{\mu U}$. It is not illogical to suppose that U ought to be approximately $\mathcal{T}/\mu$ (tension pulling the fluid along fighting viscosity slowing the fluid down), so we can then rewrite Eqn. 1.9 as

$$\left[\frac{\partial \vec{u}_i}{\partial x_j} + \frac{\partial \vec{u}_j}{\partial x_i}\right] \cdot \hat{n}_j = \tilde{P}\hat{n}_i + \kappa\hat{n}_i. \tag{1.12}$$

Now that we have these nondimensionalized equations and have made an assumption of low Reynolds number, we can begin to manipulate them to derive the lubrication equation. For instance, since we know that $\nabla \cdot \vec{u} = 0$, we can introduce a stream function ψ which is defined so that $u = -\psi_y$ and $v = \psi_x$. Note that since $\Delta u = \hat{P}_x$ and $\Delta v = \hat{P}_y$, we can say that $\Delta(u_y - v_x) = \Delta(-\psi_{yy} - \psi_{xx}) = 0$, so

$$\Delta^2\psi = 0. \tag{1.13}$$

Furthermore, by the no-slip condition, $\psi_x = \psi_y = 0$ at $y = 0$, so we can say that $\psi(x, 0) = 0$ since ψ is arbitrary up to a constant.

Then, for fixed x, we know that

$$\int_0^h u\, dy = \int_0^h -\psi_y\, dy = \psi(x,0) - \psi(x,h) = -\psi(x,h), \tag{1.14}$$

which allows us to write the kinematic condition as

$$h_t + \frac{\partial}{\partial x}\left[-\psi(x,h)\right] = 0. \tag{1.15}$$

We have nondimensionalized equations, some in terms of a stream function ψ. Now we will rescale length and time variables in order to draw conclusions about the structure of the stream function. Define two new variables X and T such that $X = \varepsilon x$ and $T = \varepsilon^3 t$, leaving $y = y$ with no rescaling, for some small $\varepsilon > 0$. Then we can use Eqn. 1.13 to write

$$\Delta^2\psi = \left[\varepsilon^2\frac{\partial^2}{\partial X^2} + \frac{\partial^2}{\partial y^2}\right]\left[\varepsilon^2\frac{\partial^2}{\partial X^2} + \frac{\partial^2}{\partial y^2}\right]\psi = 0, \tag{1.16}$$

which tells us that to within $O(\varepsilon^2)$, $\psi_{yyyy} = 0$ for all y. So we can solve for ψ as $\psi(X,y) = A(X) + B(X)y + C(X)y^2 + D(X)y^3$. But because of the no-slip condition, which says that $\psi(X,0) = 0$, we find that $A(X) = 0$. Another consequence of the no-slip condition is that $\psi_y(X,y) = 0$, so $B(X) = 0$ as well. So ψ can be written simply as $\psi(X,y) = C(X)y^2 + D(X)y^3$.

Now define a vector $\vec{R}(x) = (x, h(x,t))$ that points from the origin to the point on the surface above point x. The tangent vector $\hat{t}$ at this point is given by $\hat{t} = \frac{(1,h_x)}{\sqrt{1+h_x^2}}$, and the normal vector $\hat{n}$ is given by $\hat{n} = \frac{(-h_x,1)}{\sqrt{1+h_x^2}}$. The curvature κ is given by $\kappa = \frac{h_{xx}}{(1+h_x^2)^{3/2}}$.

Then from the tangential force balance, we can write

$$\hat{t}_i \cdot T_{ij} \cdot \hat{n}_j = (\hat{t}\cdot\hat{n})(P + \kappa) = 0. \tag{1.17}$$

But using our rescaling of the x variable as $X = \varepsilon x$, we simplify the expressions for $\hat{t}$ and $\hat{n}$ by noting that

$$\hat{t}(X) = \frac{(1, \varepsilon h_X)}{\sqrt{1+\varepsilon^2 h_X^2}}, \tag{1.18}$$

which is simply $(1,0) + O(\varepsilon)$, and we discard the terms of order ε because they are small in comparison to the other terms.. Similarly $\hat{n}(X) = (0,1) + O(\varepsilon)$. Then it is the case that

$$\begin{aligned} 0 = \hat{t}_i \cdot T_{ij} \cdot \hat{n}_j &= \frac{\partial u}{\partial y} + \frac{\partial v}{\partial x} = -\psi_{yy} + \psi_{xx} \\ &= -\psi_{yy} + \varepsilon^2\psi_{XX} \\ &= -\psi_{yy} + O(\varepsilon^2). \end{aligned} \tag{1.19}$$

This applies only at the surface where the tangential stresses are felt in the fluid, so this statement allows us to note that $0 = \psi_{yy}(X,h)$. But since $\psi(X,y) = C(X)y^2 + D(X)y^3$, we have that $0 = \psi_{yy}(X,h) = 2C(X) + 6D(X)h$, or $C(X) = -3D(X)h$. So at last we write

$$\psi(X,y) = D(X)\left[y^3 - 3y^2h\right]. \tag{1.20}$$

The above result comes from balancing the tangential stress. We will complete the derivation of the lubrication equation by balancing the normal stresses. Recall from Eqn. 1.12 that

$$\hat{n}_i \cdot \left[\frac{\partial \vec{u}_i}{\partial x_j} + \frac{\partial \vec{u}_j}{\partial x_i}\right] \cdot \hat{n}_j = (P + \kappa)(\hat{n} \cdot \hat{n}). \tag{1.21}$$

Recalling again that, because of the small-slope approximation, $\hat{n} = (0,1) + O(\varepsilon)$, we can write this constraint as

$$2\frac{\partial v}{\partial y} = P + \varepsilon^2 h_{XX}, \tag{1.22}$$

where we have substituted $\kappa = \varepsilon^2 h_{XX}$, dropping the normalizing factor of $1/(1+h_X^2)^{3/2}$ since $h_X^2 \sim O(\varepsilon^2)$. Replacing v with $\psi_x = \varepsilon\psi_X$, we then write

$$2\varepsilon\psi_{Xy} = P + \varepsilon^2 h_{XX}. \tag{1.23}$$

But then we note that

$$P_x = \Delta u = -\Delta\psi_y = -\psi_{yyy} + O(\varepsilon^2), \tag{1.24}$$

so that

$$\varepsilon P_X = -\psi_{yyy}. \tag{1.25}$$

If we then take the X derivative of Eqn. 1.23, we are left with

$$2\varepsilon^2\psi_{XXy} = \varepsilon P_X + \varepsilon^3 h_{XXX}, \tag{1.26}$$

which becomes

$$\varepsilon^3 h_{XXX} = -\psi_{yyy} + O(\varepsilon^2). \tag{1.27}$$

But we also know from the tangential stress balance that $\psi_{yyy} = 6D(X)$, so we conclude that $6D(X) = -\varepsilon^3 h_{XXX}$, which allows us to write the stream function ψ as

$$\psi(X,y) = -\frac{\varepsilon^3}{6} h_{XXX}\left[y^3 - 3y^2h\right], \tag{1.28}$$

which at $y = h$ becomes

$$\psi(X,h) = \frac{\varepsilon^3}{3} h^3 h_{XXX}. \tag{1.29}$$

Recall now the kinematic condition written in terms of the stream function, Eqn. 1.15. Plugging in the final equation for the stream function, and recalling that we rescaled $T = \varepsilon^3 t$, we obtain at long last

$$\varepsilon^3 \left[h_T + \partial_X \left(\frac{h^3}{3} h_{XXX} \right) \right] = 0, \tag{1.30}$$

which (when the ε^3 is removed) is the lubrication equation. The driving term is the pressure gradient, which balances the curvature that arises as a result of the film's surface tension.

The h^3 term is known as the *mobility* of the film. It is, in a sense, a measure of the friction created by the viscosity as the fluid drags itself along, and its form is specified by the geometry of the fluid. This is the effect we remarked on early on when describing the meaning of different exponents n in the thin film equation. So, for instance, the mobility of a fluid in a Hele-Shaw cell is h, since $n = 1$ for such a fluid.

1.1.2 Terms and Definitions

We say that the film has *ruptured* if $h(x,t) = 0$ for any x, t.

A rupture is *finite-time* if for some $T < \infty$ and $X \in \Omega$ (where Ω is the domain of interest), $h(X,T) = 0$ and *infinite-time* if for some $X \in \Omega$, $lim_{t\to\infty} h(X,t) = 0$ but the conditions for finite-time rupture are not satisfied. A rupture may also be called a *singularity*.

If, for certain boundary conditions and exponents n, there is a quantity of fluid present above which the film experiences rupture and below which it does not, we call this quantity the *critical mass*.

A quantity Q is said to be *conserved* if $\frac{dQ}{dt} = 0$. Similarly, the quantity Q is said to be *dissipated* if $\frac{dQ}{dt} \leq 0$.

1.2 The Problems

Consider a bounded domain $\Omega = [-L, L]$. The thin film equation is fourth-order in the spatial variable and first-order in the temporal variable, so in order for the thin film equation to be well-posed on this domain, we must

specify two boundary conditions at each endpoint $x = \pm L$ and we must also specify the initial position $h(x, 0) = h_0(x)$.

It is common, for instance, to impose periodic boundary conditions on the film so that any boundary terms resulting from integration by parts are irrelevant.

It is also common to consider a spreading-droplet solution, for which $h(x, t) = 0$ at the boundary and for which h can actually be expressed as a function of t multiplied by a function of a single similarity variable.

We might also fix the height of the film at the boundary and consider pressure boundary conditions, for which $h_{xx}(\pm L) = p$, which is equivalent to a constant external pressure, or current boundary conditions, for which $h_{xxx}(\pm L) = \pm c$, which describes liquid draining out of a region at a constant rate. Both of these types of boundary conditions are treated briefly in Bertozzi (1996).

Note 1.1. *We are concerned with solutions of the thin film equation for which* $h(x, t) \geq 0$ *for all* x, t*. The positivity (or non-negativity) of solutions is discussed extensively in Bertozzi (1998).*

Of primary concern in the study of the thin film equation is the investigation of the film's singularities. We are particularly concerned about this investigation for two reasons. First, the physical applications of lubrication theory often depend on the film remaining intact throughout some industrial process, e.g. the application of a UV-protectant film to a pair of sunglasses. Second, while the behavior of a fluid under the thin film equation is generally quite complex, the question of whether a film does or does not rupture is much simpler to grasp, and is tractable to both theoretical and numerical methods.

1.3 Prior Research

Although this particular branch of fluid dynamics is relatively young, there is already a significant body of work describing results related to the thin film equation itself or to thin-film-type equations generally.

A good first summary of the main results in lubrication theory is given in Bertozzi (1998), which presents an overview of the nature of thin films and discusses in depth the problem of contact lines and interfaces, which ultimately motivates this research. It also illustrates some of the more familiar recent results and methods, such as characterization of some types

of finite-time singularities. Finally, it contains a summary of energy arguments (see Sec. 2.2) for the impossibility of singularities in certain cases, including an extended discussion on the possibility that there is a specific critical exponent above which the film cannot rupture and that it is unclear whether or not such an exponent would depend on the boundary conditions of the film.

Although this paper considers only the surface tension term of the thin film equation, it is quite common to reintroduce other terms that describe other governing forces of the flow, e.g. gravity, van der Waals forces, thermocapillarity, and so forth. Oron et al. (1997) is one thorough review of these topics, and Myers (1998) is another, with many physical examples in which these forces come into play.

The porous medium equation $h_t = \nabla \cdot (h^n \nabla h)$ can serve as a template for means of investigating the thin film equation, as in Carrillo and Toscani (2002), in which the authors use techniques from the study of the porous medium equation to show that spreading-droplet solutions of the thin film equation with $n = 1$ decay to the unique strong source-type solution of equivalent mass.

In further results relating to source-type solutions of the thin film equation, Bernoff and Witelski (2002) discusses source-type solutions for $0 < n < 3$ in terms of similarity variables and proves that these solutions are stable. This paper also gives the eigenvalue spectrum and associated eigenfunctions for the $n = 1$ case using the fact that the similarity equation has an exact polynomial solution.

It is also sometimes profitable to examine self-similar singularities of the film, as in Bertozzi (1996), in which power series are used to investigate the behavior of similarity solutions both for the thin film equation and for the modified thin film equation $h_t + h^n h_{xxxx} = 0$. This paper also presents results concerning the values of the exponent n for which the modified equation experiences a finite-time singularity and for which it experiences infinite-time singularity. This question is of some interest in the study of the unmodified equation, but as yet no significant results are forthcoming.

In the category of results most pertinent to our own research, Laugesen (2004) describes integrals of the form $\int h^p h_x^2 dx$ and shows that they are dissipated for certain values of p and n; that is, that their time derivatives are nonpositive for all t. Further discussion of integrals similar to this and their behavior follows in Sec. 2.2. Laugesen also shows that rupture of the film is impossible for certain values of n; this proof follows in Sec. 1.4.

Conversely, for some boundary conditions it can be shown that for certain values of n rupture not only *can* occur but *must* occur. There are far

fewer results of this type in the literature than there are results describing situations in which rupture cannot occur, and these results seem to be concentrated in the study of the Hele-Shaw cell, for which $n = 1$. Most studies of this problem approach it from a numerical standpoint (as in Almgren (1996), Constantin et al. (1993), and Dupont et al. (1993)), though it is also possible to use the asymptotics of the region near the rupture (as in Almgren et al. (1996)).

A proof that rupture must occur for pressure boundary conditions for $0 < n < 1/2$ appears in Beretta et al. (1995); in Sec. 2.7 we present one for our own boundary conditions. While our proof is not as richly analytical as the proof in Beretta et al. (1995), it has a more evident physical origin and a more intuitive mechanism.

In Bertozzi (1998), a numerical scheme is presented for solving the thin film equation; this and similar schemes are expanded upon in Zhornitskaya and Bertozzi (2000) and demonstrated to be positivity-preserving. The schemes are also shown to preserve stability and convergence, which is to say that they do not exhibit false rupture of the film but in fact remain close to the true solution. Curiously, for periodic boundary conditions, this scheme can be proven never to experience rupture for $n \geq 2$, whereas the strongest unqualified theoretical result can only establish $n > 7/2$. There are theoretical results, as shown in Bertozzi et al. (1994), that indicate that *if* it can be shown that h_{xx} is bounded for all time, then there can in fact be no rupture for $n \geq 2$, but this boundedness has not been proven.

Bertozzi (1996) also uses numerical schemes to support some of the results achieved in that paper, discussed above in 1.3; for instance, simulations are used to compare similarity shape of singularities and the time dependence of the minimum thickness of the film to the theoretical predictions. This is similar to the refinement analysis we will describe in Sec. 3.3.

1.4 A Prior No-Rupture Proof

Since the determination of whether or not a film ruptures is the problem of primary importance in the study of the thin film equation, it may be worthwhile to reproduce a preexisting characterization of instances in which it is impossible for the film to rupture. The following proof is due to Laugesen in Laugesen (2004), though the first proof of this result was given ten years earlier in Bertozzi et al. (1994). I will trace the high points of Laugesen's version of the proof, with explanations of the key steps.

Theorem 1.1. *(Laugesen 2004; Bertozzi, Kadanoff, et al., 1994) Suppose that $h(x,t)$ solves the thin film equation $h_t = -(h^n h_{xxx})_x$ with periodic boundary conditions and $h(x,0) > 0$. Then h cannot experience rupture for $n > 3.5$.*

Proof. Define the quantities $E = \int_\Omega h_x^2 \, dx$ and $P_m = \int_\Omega h^m \, dx$. Then by the Cauchy-Schwarz inequality, we know that

$$\begin{aligned} \sqrt{EP_m} &\geq \int_\Omega \left| h^{m/2} h_x \right| \, dx \\ &= C \int_\Omega \left| \frac{\partial}{\partial x} h^{m/2+1} \right| \, dx, \end{aligned}$$

where $C = 1/|m/2+1|$. We also know that in general, for a periodic function f,

$$\int_\Omega |f_x| \, dx \geq \max(f) - \min(f),$$

so for $f_x = h^{m/2+1}$ we conclude that

$$\sqrt{EP_m} \geq C[\max(h^{m/2+1}) - \min(h^{m/2+1})].$$

Now suppose that $m/2+1 < 0$ and that E and P_m are bounded. Then we know that $\max(h) > \bar{h}$, where $\bar{h}$ is the average value of h, so since $m/2+1 < 0$, we know that $\min(h^{m/2+1}) < \bar{h}^{m/2+1}$, which is constant.

Therefore $C\min(h^{m/2+1}) + \sqrt{EP_m}$ is bounded and thus $\max(h^{m/2+1})$ is bounded since

$$\min(h^{m/2+1}) + \frac{1}{C}\sqrt{EP_m} \geq \max(h^{m/2+1}).$$

If it were the case that $h \to 0$, we would have $h^{m/2+1} \to \infty$ since $m/2+1 < 0$. But $h^{m/2+1}$ is bounded, so this cannot be the case. Therefore the film cannot rupture.

As Laugesen points out, prior work in Bertozzi et al. (1994) has shown that $\int h^{q+3/2-n} dx$ is dissipated for $q = 0$. Considering this integral as an instance of P_m with $m = q + 3/2 - n$, once we set $q = 0$ and make use of the fact that rupture cannot occur when $m/2+1 < 0$, basic arithmetic shows that rupture cannot occur for $n > 3.5$.

□

This proof is generally representative of the style common to most proofs of rupture or no rupture. The integral estimates, Cauchy-Schwarz inequality, and bounding arguments are common elements. Unfortunately, this

proof also makes use of one convenient fact which we cannot: because the boundary conditions were specified to be periodic, the boundary terms vanish that result from the integration by parts that allows Laugesen (and earlier Bertozzi, Kadanoff, et al.) to determine when $\int h^{q+3/2-n}\,dx$ is dissipated. We do not have this luxury, as will become clear presently.

Chapter 2

Theory

2.1 Our Model

2.1.1 Physical Basis: Surface Chemistry

In section 1.2, we presented a number of possible boundary conditions for thin films, including periodic, pressure, and current boundary conditions. We are concerned with a different set of conditions; in particular, we consider those which represent films exhibiting a thin capillary meniscus. That is, we consider a fluid on a solid substrate with walls on either side and covered above by a vapor or other less dense fluid, and we suppose that the fluid has some fixed contact angle θ with the walls. If $\theta < 90^\circ$, we say that the fluid *wets* the walls; if $\theta > 90^\circ$, we say that the fluid *does not wet* the walls. In the special case when $\theta = 0^\circ$, we say that the film is *perfectly wetting*.

For a given combination of fluid, covering vapor, and material making up the walls, the contact angle is given by *Young's Law*,

$$\gamma_{sv} - \gamma_{sl} - \gamma_{lv} \cos\theta = 0 \tag{2.1}$$

where γ_{sv}, γ_{sl}, and γ_{lv} are the solid/vapor, solid/liquid, and liquid/vapor *interfacial energies* or *surface tensions*. Since interfacial energies have units of energy per unit area, which is force per unit length, Young's equation can be derived from balance of forces in Fig. 2.1.

While many chemists and physicists interested in the behavior of surfaces are interested in contact angles, the angle θ may vary with the temperature at which measurements are taken, the purity of the liquid, the cleanliness of the solid material of the walls, and numerous other variable

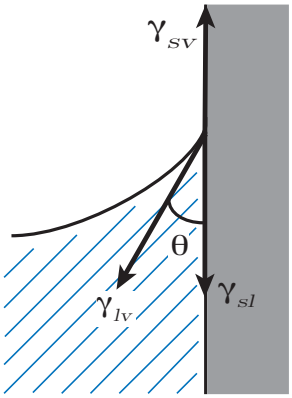

Figure 2.1: Solid, liquid, and vapor interfaces at the contact line.

factors. For this reason, contact angles are not tabulated, though it is often possible to generally describe the behavior of a given fluid on a given substrate, e.g. very pure water on very clean borosilicate glass is approximately perfectly wetting, whereas pure water tends to bead up rather than wetting Teflon.

2.1.2 Mathematical Representation

We consider films in one spatial and one temportal dimension over a finite spatial interval $\Omega = [-L, L]$. Rather than actually setting the contact angle at the boundary, we consider a slope of fixed magnitude, so that $h_x(\pm L) = \pm\alpha$. As an aid to intuition, the value α is positive when it is energetically favorable for the film to wet the surface and negative when it is not. To reflect the presence of walls at the boundary, we also set $h_{xxx}(\pm L) = 0$, representing a condition of no mass flux.

Mathematically, we state the full problem as follows:

$$\begin{aligned} h_t + (h^n h_{xxx})_x &= 0; \\ h_x(\pm L, t) &= \pm\alpha; \\ h_{xxx}(\pm L, t) &= 0; \\ h(x, 0) &= h_0(x). \end{aligned}$$

Fig. 2.1.2 shows two pictures of thin films with different contact angles, to illustrate how the choice of α affects the eventual shape of the film.

Note 2.1. *Although we typically set $\theta \neq 0$ at the walls, we always assume that the fluid is perfectly wetting along the line $h = 0$ (on the floor of the film's container).*

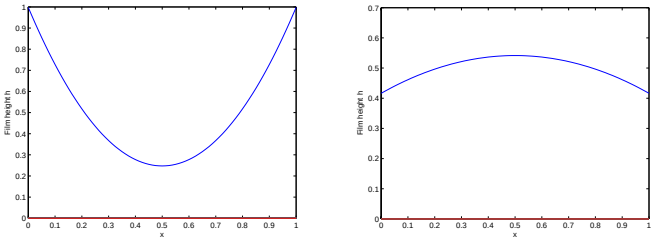

(a) A meniscus with $\alpha = 3$ (b) A meniscus with $\alpha = -.5$

Figure 2.2: Examples of films with positive and negative contact angle.

This assumption is a necessary fact of the no-slip condition, which would prevent the fluid fronts from propagating if a dry spot ever formed without perfect wetting at the edges of the dry spot. A number of modifications to the model have been proposed to account for this unfortunate non-physical mathematical result, but they are beyond the scope of this work.

2.2 Energies

The primary theoretical method for attacking the behavior of the thin film equation is to consider quantities related to the film which we call *energies*. Some of these energies have a definite physical relationship with the film, while others need not. The investigation of whether these energies are conserved or dissipated can help us describe the film. Energies are sometimes also called *entropies*.

2.2.1 Mass

In a physical calculation, we could define the mass of the film as

$$\text{Mass} = \int \rho \, dV = \int_\Omega \rho h \, dx, \tag{2.2}$$

where ρ, the density of the film, is constant due to the assumption that the film is incompressible. Since our primary interest in energies is in whether they are conserved or dissipated, and the presence or absence of positive multiplicative constants does not affect this behavior, we can safely disre-

gard ρ in all our calculations and define mass simply as

$$M = \int_\Omega h \, dx. \tag{2.3}$$

Since we have specified no-flux conditions at the boundary, we do not expect a change in mass as the film evolves over time. It is quick to prove that mass is in fact conserved for the thin film equation for our boundary conditions.

Theorem 2.1. *For the thin capillary meniscus, mass is conserved.*

Proof. The proof is by straightforward calculation:

$$\begin{aligned} \frac{\partial}{\partial t} M &= \int_\Omega h_t \, dx \\ &= \int_\Omega -(h^n h_{xxx})_x \, dx \\ &= -h^n h_{xxx}|_{-L}^{L} \\ &= 0, \end{aligned}$$

since $h_{xxx}(\pm L) = 0$. Therefore $\frac{\partial}{\partial t} M = 0$ and thus mass is conserved. □

2.2.2 Surface Area

The arclength of a function $f : \mathbb{R} \to \mathbb{R}$ between two points $x = a$ and $x = b$ is given by

$$\text{Arclength} = \int_a^b \sqrt{1 + (f')^2} \, dx. \tag{2.4}$$

Since we assume that $|h_x| \ll 1$, we can instead write

$$\text{SurfaceArea} = \int_\Omega \sqrt{1 + h_x^2} \, dx = \int_\Omega 1 + \frac{h_x^2}{2} \, dx \tag{2.5}$$

using a Taylor expansion. The factor of $1/2$, like ρ above, is a positive constant that does not affect our calculations, and the additive constant of 1 ($2L$ once integrated) disappears when we take the time derivative, so we disregard it as well. This allows us to define the surface area simply as

$$SA = \int_\Omega h_x^2 \, dx. \tag{2.6}$$

It is also possible to show that surface area is dissipated, but we will postpone a mathematical argument for now in favor of a thermodynamical

one. A system's most stable state is that state for which the Gibbs free energy is minimized. It can be demonstrated that any addition of surface area A for a surface with tension γ introduces an additional (positive) term γA in the Gibbs free energy, so the Gibbs free energy is minimized when the surface area is as small as possible. The minimal possible surface area for a fluid between two walls occurs for a flat film—the quantity h_x^2 is always non-negative, and is minimized when $h_x = 0$.

2.2.3 Coating Energy

We are concerned with the behavior of a film exhibiting a thin capillary meniscus. If we consider only mass and surface area, we would expect the film to converge to a flat solution, as this minimizes surface area. Real-world observation indicates, however, that this is clearly not the case. (Films *can* be flat or close to flat, if γ_{sv} and γ_{sl} are the same or very close, since this forces $\gamma_{lv} \cos\theta \approx 0$ or $\theta \approx 90^\circ$ in Eqn. 2.1, but for the most part we observe meniscus behavior instead.) We use coating energy to explain the existence of capillary behavior.

We intuitively define coating energy as a measure of the fluid's "desire" to stick to the walls of the box we put it in. Recalling that $\pm\alpha$ is the slope of the film at $\pm L$, defining the contact angle of the film with the boundary, the coating energy is $\alpha h|_{-L}^{L}$. With the physical intuition that the fluid likes to coat the walls, we suppose that the coating energy decreases the overall energy of the film (makes the configuration more energetically favorable), so we define an energy in which surface area and coating energy balance each other, as follows:

$$E = \frac{1}{2}\int_\Omega h_x^2 \, dx - \alpha h|_{-L}^{L}.$$

Theorem 2.2. *For a thin capillary meniscus, E is dissipated.*

Proof. Consider $\frac{\partial}{\partial t}E$ and note that

$$\begin{aligned}
\frac{\partial}{\partial t}E &= \frac{\partial}{\partial t}\left[\int_\Omega h_x^2/2 \, dx - \alpha h|_{-L}^{L}\right] \\
&= \int_\Omega h_x h_{xt} \, dx - \alpha h_t|_{-L}^{L} \\
&= -\int_\Omega h_x (h^n h_{xxx})_{xx} \, dx - \alpha h_t|_{-L}^{L},
\end{aligned}$$

in which we differentiate freely under the integral sign and rearrange partial derivatives because solutions to the thin film equation before rupture

must be at least $C^4(\Omega)$ (in fact, $h^n h_{xxx}$ is well-behaved). We also replace $h_t = -(h^n h_{xxx})_x$. Integrating by parts twice, we get

$$\begin{aligned}\frac{\partial}{\partial t}E &= -\int_\Omega \left[h^n h_{xxx}^2 - [h_x(h^n h_{xxx})_x - h_{xx}h^n h_{xxx}]|_{-L}^{L}\right]\, dx - \alpha h_t|_{-L}^{L} \\ &= -\int_\Omega h^n h_{xxx}^2\, dx + h_x h_t|_{-L}^{L} - \alpha h_t|_{-L}^{L} \\ &= -\int_\Omega h^n h_{xxx}^2\, dx\end{aligned}$$

Since $h(x,t) \geq 0$ for all x, t, this integrand is everywhere non-negative, and therefore $\frac{\partial}{\partial t}E \leq 0$, showing that E is dissipated. □

2.3 Minimizers

For energies which are dissipated over time, we would like to know what form the film takes when it has achieved the steady state; that is, how to express the *minimizer* of a particular energy. For some energies this is simple; consider the pure surface energy expression and note that the integral is minimized when $h_x = 0$ for all x, so that assuming surface energy is the only thing driving the film's behavior, the minimizer is a flat film.

However, flat films do not fit our meniscus boundary conditions, in which we generally set the contact angle to be something nonzero. (Nothing prevents us from considering the $\alpha = 0$ case, but it is not particularly interesting or informative.) So we instead consider the coating energy of the film and attempt to find the film that minimizes the energy E, described above in Sec. 2.2.3. It is in fact the case that for given boundary conditions (and exponents n for which rupture may occur) there is a so-called *critical mass*; this is the mass M_c such that if the film has a mass greater than M_c, then there is sufficient fluid that the film will not rupture, but if the film has a mass less than M_c, the film will rupture. We will compute M_c in a moment, after a preliminary result.

Theorem 2.3. *Assuming the mass of the film is above the critical mass (so there is no danger that the film will rupture), and noting that mass is conserved as we have previously shown, the minimizer of the energy* $E = (1/2)\int_\Omega h_x^2\, dx - \alpha h|_{-L}^{L}$ *is a quadratic of the form* $\bar{h}(x) = \frac{\alpha x^2}{2L} + b$.

Proof. Consider the function $\bar{h}(x) = \frac{\alpha x^2}{2L} + b$, where the value of the constant b depends on the mass of the fluid. Then consider a small perturbation δ of the fluid; this perturbation must be massless in order that mass be

conserved overall. Also consider E as a function of the perturbation; that is, $E(\delta)$ is the energy of a given film $h = \bar{h} + \delta$, and $E(0)$ is the energy of $\bar{h}$. To show that $\bar{h}$ is a minimizer, it suffices to show that $E(\delta) \geq E(0)$.

$$\begin{aligned}
E(\delta) - E(0) &= \frac{1}{2}\int_\Omega \left[\left(\frac{\alpha x^2}{2L} + b + \delta\right)_x^2 - \left(\frac{\alpha x^2}{2L} + b\right)_x^2\right] dx \\
&\quad -2\alpha\left(\frac{\alpha L}{2} + b + \delta\right) + 2\alpha\left(\frac{\alpha L}{2} + b\right) \\
&= \frac{1}{2}\int_\Omega \left[\left(\frac{\alpha x}{L} + \delta_x\right)^2 - \left(\frac{\alpha x}{L}\right)^2\right] dx - 2\alpha\delta \\
&= \frac{1}{2}\int_\Omega \left[\frac{2\alpha x\delta_x}{L} + \delta_x^2\right] dx - 2\alpha\delta \\
&= \int_\Omega \frac{\delta_x^2}{2}\, dx + \frac{\alpha x\delta}{L}\bigg|_{-L}^{L} - \int_\Omega \frac{\alpha\delta}{L}\, dx - 2\alpha\delta \\
&= \int_\Omega \frac{\delta_x^2}{2}\, dx,
\end{aligned}$$

since, as we said, δ is massless, so $\int_\Omega (\alpha\delta)/L\, dx = 0$. But $\delta_x^2 \geq 0$, so $E(\delta) - E(0) \geq 0$ and therefore $\bar{h}$ must be a minimizer of the energy E. □

Now we are equipped to compute the critical mass of the fluid.

Theorem 2.4. *The critical mass of fluid in a thin capillary meniscus in a domain $[-L, L]$ with contact angle α is $\alpha L^2/3$.*

Proof. We just proved that the minimizer of the coating energy has the form $\bar{h}(x) = \alpha x^2/(2L) + b$. The smallest possible mass such a quadratic can have and not experience rupture is the mass of the fluid for which the minimum of the quadratic just touches down on the x-axis; this must be the critical mass M_c. In this case, the equation for the minimizer is $\bar{h}(x) = \alpha x^2/(2L)$, since the minimum of the parabola must by symmetry occur at $x = 0$ and contact with the x-axis thus implies that $b = 0$.

Now we can quickly integrate $\bar{h}$ to find the critical mass:

$$M_c = \int_{-L}^{L} \frac{\alpha x^2}{2L}\, dx = \frac{\alpha x^3}{6L}\bigg|_{-L}^{L} = \frac{\alpha L^2}{3}.$$

□

If we suppose that the film is below critical mass and therefore experiences a dry spot in the interior, we must formulate the minimizer slightly

differently. Particularly, the curve must touch down smoothly on either side of the dry spot to preserve the continuity of the derivative. Therefore we claim the following result.

Theorem 2.5. *Assuming that the film is below critical mass and therefore touches down at two points, the minimizer of the energy E is actually symmetric; if we call the touchdown points $-l$ and l, the minimizer can be defined as*

$$\bar{h}(x) = \begin{cases} \frac{\alpha(x+l)^2}{2(L-l)} & 0 \le x \le -l \\ 0 & -l \le x \le l \\ \frac{\alpha(x-l)^2}{2(L-l)} & l \le x \le L \end{cases}$$

Proof. As above, let $h = \bar{h} + \delta$, where δ is some perturbation, and consider $E(\delta)$ to be the energy of h, while $E(0)$ is the energy of $\bar{h}$. If we can show that $E(\delta) > E(0)$ for any δ, this shows that $\bar{h}$ is a minimizer of the energy E. We proceed by direct computation.

$$\begin{aligned}
E(\delta) - E(0) &= \int_{-L}^{L} \frac{h_x^2}{2}\,dx - \alpha h|_{-L}^{L} - \int_{-L}^{L} \frac{\bar{h}_x^2}{2}\,dx + \alpha \bar{h}|_{-L}^{L} \\
&= \int_{-L}^{l} \frac{1}{2}\left(\frac{\alpha(x+l)}{2(L-l)} + \delta_x\right)^2 dx + \int_{-l}^{l} \frac{\delta_x^2}{2}\,dx \\
&\quad + \int_{l}^{L} \frac{1}{2}\left(\frac{\alpha(x-l)}{(L-l)} + \delta_x\right)^2 dx \\
&\quad - \alpha\left(\frac{\alpha(L+l)}{2} + \delta(L) + \frac{\alpha(l-L)}{2} - \delta(-L)\right) \\
&\quad - \int_{-L}^{l} \frac{1}{2}\left(\frac{\alpha(x+l)}{2(L-l)}\right)^2 dx + \int_{-l}^{l} 0^2\,dx + \int_{l}^{L} \frac{1}{2}\left(\frac{\alpha(x-l)}{(L-l)}\right)^2 \\
&\quad + \alpha\left(\frac{\alpha(L+l)}{2} + \frac{\alpha(l-L)}{2}\right) \\
&= \int_{-L}^{l} \left(\frac{\alpha(x+l)\delta_x}{(L-l)} + \frac{\delta_x^2}{2}\right) dx + \int_{-l}^{l} \frac{\delta_x^2}{2}\,dx \\
&\quad + \int_{l}^{L} \left(\frac{\alpha(x-l)\delta_x}{(L-l)} + \frac{\delta_x^2}{2}\right) dx - \alpha\delta(L) + \alpha\delta(-L) \\
&= \int_{-L}^{L} \frac{d_x^2}{2}\,dx + \frac{\alpha(x+l)\delta}{(L-l)}\bigg|_{-L}^{l} - \int_{-L}^{-l} \frac{\alpha\delta}{(L-l)}\,dx \\
&\quad + \frac{\alpha(x-l)\delta}{(L-l)}\bigg|_{l}^{L} - \int_{l}^{L} \frac{\alpha\delta}{(L-l)}\,dx - \alpha\delta(L) + \alpha\delta(-L) \\
&= \int_{-L}^{L} \frac{\delta_x^2}{2}\,dx - \int_{-L}^{-l} \frac{\alpha\delta}{(L-l)}\,dx - \int_{l}^{L} \frac{\alpha\delta}{(L-l)}\,dx
\end{aligned}$$

Now, we know that mass is conserved, so δ is massless, or

$$\int_{-L}^{L} \delta \, dx = 0.$$

Therefore

$$\frac{\alpha}{(L-l)} \int_{-L}^{L} \delta \, dx = 0,$$

meaning

$$\int_{-l}^{l} \frac{\alpha\delta}{(L-l)} \, dx = -\int_{-L}^{-l} \frac{\alpha\delta}{(L-l)} \, dx - \int_{l}^{L} \frac{\alpha\delta}{(L-l)} \, dx.$$

So we see that

$$E(\delta) - E(0) = \int_{-L}^{L} \frac{\delta_x^2}{2} \, dx + \int_{-l}^{l} \frac{\alpha\delta}{(L-l)} \, dx.$$

Now, clearly $\int_{-L}^{L} \frac{\delta_x^2}{2} \, dx \geq 0$. Furthermore, δ is the height of $h = \bar{h} + \delta$ on $[-l, l]$ since $\bar{h} = 0$ on $[-l, l]$. Then δ is nonnegative on $[-l, l]$ since film heights cannot be negative. So $\int_{-l}^{l} \frac{\alpha\delta}{(L-l)} \, dx \geq 0$ as well. Therefore

$$E(\delta) - E(0) \geq 0,$$

and thus $\bar{h}$ is a (global) minimizer of the energy E.

□

2.4 Boundedness

It is not immediately obvious that the height of the film in a thin capillary meniscus must be bounded, though it is perhaps intuitive. We can prove that the film thickness is, in fact, bounded using energy methods.

Theorem 2.6. *If $h(x,t)$ solves $h_t = -(h^n h_{xxx})_x$ on $\Omega = [-L, L]$ with $h_x = \pm\alpha$ and $h_{xxx} = 0$ at the boundary, then $h(x,t) < \infty$ for all x, t.*

Proof. Consider the energies

$$E = \int_{\Omega} h_x^2 \, dx - \alpha h|_{-L}^{L} \qquad \text{and} \qquad M = \int_{\Omega} h \, dx$$

Now consider their product and apply the Cauchy-Schwarz Inequality:

$$EM = \int_{\Omega} h_x^2 \, dx \int_{\Omega} h \, dx - M\alpha h|_{-L}^{L} \quad \geq \quad \int_{\Omega} |h_x h^{1/2}| \, dx - M\alpha h|_{-L}^{L}$$

$$\begin{aligned} &= \frac{2}{3}\int_\Omega \left|\frac{\partial}{\partial x}h^{3/2}\right| \, dx - M\alpha h|_{-L}^{L} \\ &\geq \frac{2}{3}\max(h^{3/2}) - M\alpha h|_{-L}^{L}, \end{aligned}$$

noting in the last step that $\int_\Omega |f_x| \, dx \geq \max(f) - \min(f)$ for any f and that $\min(h) = 0$.

Then consider that $E(0) > E(t)$ for all t, since E is dissipated. Furthermore, $2M\alpha \max(h) \geq M\alpha h|_{-L}^{L}$, so we have the following expression after rearranging the last inequality above:

$$E(0)M + 2M\alpha \max(h) \geq \frac{2}{3}\max(h^{3/2}) \tag{2.7}$$

But $h^{3/2}$ dominates h as $h \to \infty$, so since $E(0)M$ is a constant, Eqn. 2.7 is a contradiction if $h \to \infty$. Therefore h must be bounded. □

2.5 No Rupture

Just as Laugesen showed that rupture cannot occur in a film with periodic boundary conditions for $n \geq 3.5$, we can obtain a similar (albeit somewhat weaker) result for the thin capillary meniscus.

Theorem 2.7. *Assuming that h_{xx} is bounded for all t and that the energy given by $P_m = \int_\Omega h^m \, dx$ is bounded, there can be no rupture in a thin capillary meniscus for $m < -2$.*

Proof. Consider the thin film equation with capillary meniscus boundary conditions, and consider the energies

$$E = \int_\Omega h_x^2 \, dx - \alpha h|_{-L}^{L} \qquad \text{and} \qquad P_m = \int_\Omega h^m \, dx$$

Multiplying these two quantities together and applying the Cauchy-Schwarz inequality, we find that

$$\begin{aligned} EP_m &= \int_\Omega h_x^2 \, dx \int_\Omega h^m \, dx - \alpha h|_{-L}^{L} \cdot P_m \\ &\geq \left(\int_\Omega |h_x h^{m/2}| \, dx\right)^2 - \alpha h|_{-L}^{L} \cdot P_m \end{aligned}$$

Now note that $|h_x h^{m/2}| = C\left|\frac{\partial}{\partial x}h^{m/2+1}\right|$, where $C = 1/|1 + m/2|$, so

$$EP_m \geq \left(C\int_\Omega \left|\frac{\partial}{\partial x}h^{m/2+1}\right| \, dx\right) - \alpha h|_{-L}^{L} \cdot P_m$$

Furthermore, for all piecewise differentiable f, we know that $\int_\Omega |f_x|\,dx \geq \max(f) - \min(f)$, so

$$EP_m \geq \left(C(\max(h^{m/2+1}) - \min(h^{m/2+1})\right)^2 - \alpha h|_{-L}^{L} \cdot P_m. \tag{2.8}$$

Now suppose that E and P_m are bounded (see Thm. 2.8), and note that we proved in Theorem 2.6 above that h is bounded, for instance by $\max(h)$.

Using this fact and rearranging terms in Eqn. 2.8, we see that

$$EP_m + 2\alpha \max(h) \cdot P_m \geq \left(C\left[\max(h^{m/2+1}) - \min(h^{m/2+1})\right]\right)^2$$

Since the right-hand side is a perfect square, both sides of this inequality are nonnegative, and therefore we can take square roots of both sides. Also note that E is dissipated, and that therefore $E(0) \geq E(t)$ for all $t > 0$, so we can replace the function E with the constant $E(0)$ while preserving the inequality. Therefore we have

$$\sqrt{(E(0) + 2\alpha \max(h)) \cdot P_m} \geq \max(h^{m/2+1}) - \min(h^{m/2+1})$$

Again we can rearrange terms and finally see that

$$\sqrt{(E(0) + 2\alpha \max(h)) \cdot P_m} + \min(h^{m/2+1}) \geq \max(h^{m/2+1}).$$

Suppose that $m/2 + 1 < 0$. We know that both terms on the left-hand side of the inequality are bounded, the first term because we supposed all values involved were bounded, the second because

$$\min(h^{m/2+1}) \leq (\max h)^{m/2+1},$$

which is a constant since h is bounded above. Therefore $\max(h^{m/2+1})$ is bounded. If it were the case that $h \to 0$ for any x, t, we would have $h^{m/2+1} \to \infty$ since $m/2 + 1 < 0$. Therefore it cannot be the case that $h \to 0$, and thus a thin capillary meniscus cannot rupture for $m < -2$. □

Note that in the process of this proof we assumed that P_m was bounded. This has not been shown, and in fact P_m is not bounded for certain values of m. We must calculate the values of m for which P_m *is* bounded.

Furthermore, this calculation will allow us to find values of n for which no rupture can occur, which are more valuable to us than values of m for which this is the case, since n is directly involved in the thin film equation itself.

Theorem 2.8. *$P_m = \int_\Omega h^m\,dx$ is dissipated for $2 \le m+n \le 3$, assuming $h_{xx}(L)$ is bounded for all t.*

Proof. Consider $\frac{\partial}{\partial t}P_m$. With copious use of integration by parts, we can carry out the following calculation:

$$\begin{aligned}
\frac{\partial}{\partial t}P_m &= \frac{\partial}{\partial t}\int_\Omega h^m\,dx = \int_\Omega m h^{m-1}h_t\,dx \\
&= -m\int_\Omega h^{m-1}(h^n h_{xxx})_x\,dx \\
&= -m\left[h^{m-1}h^n h_{xxx}|_{-L}^{L} - (m-1)\int_\Omega h^{m-2}h_x h^n h_{xxx}\,dx\right] \\
&= m(m-1)\int_\Omega h^{m+n-2}h_x h_{xxx}\,dx \\
&= m(m-1)\int_\Omega h^{m+n-2}\left[\frac{\partial}{\partial t}(h_x h_{xx}) - h_{xx}^2\right]\,dx \\
&= -m(m-1)\int_\Omega h^{m+n-2}h_{xx}^2\,dx + \\
&\quad m(m-1)\left[h^{m+n-2}h_x h_{xx}|_{-L}^{L} - (m+n-2)\int_\Omega h^{m+n-3}h_x^2 h_{xx}\,dx\right] \\
&= m(m-1)h^{m+n-2}h_x h_{xx}|_{-L}^{L} \\
&\quad -m(m-1)\int_\Omega h^{m+n-2}h_{xx}^2 - (m+n-2)h^{m+n-3}h_x^2 h_{xx}\,dx
\end{aligned}$$

Considering the second term (let's call it I) in this integral separately for ease of calculation, we find that

$$\begin{aligned}
I &= \int_\Omega h^{m+n-3}h_x^2 h_{xx}\,dx \\
&= h^{m+n-3}\frac{h_x^3}{3}|_{-L}^{L} - \frac{m+n-3}{3}\int_\Omega h^{m+n-4}h_x^4\,dx
\end{aligned}$$

Now, putting this new expression for I back into the original expression for the derivative of P_m and assuming symmetry, we finally see that

$$\begin{aligned}
\frac{1}{m(m-1)}\frac{\partial}{\partial t}P_m &= \int_\Omega -h^{m+n-2}h_{xx}^2 + \frac{(m+n-2)(m+n-3)}{3}h_x^4\,dx \\
&\quad + 2\alpha h^{m+n-2}(L)h_{xx}(L) + 2(m+n-2)\frac{\alpha^3}{3}h^{m+n-3}(L).
\end{aligned}$$

If we want P_m to be bounded and dissipated, we need the second term in the integral to be negative and we need the boundary terms outside the integral to remain bounded. Therefore we need $h_{xx}(L)$ to be bounded, which we in fact assumed for the purposes of this proof, and we need $(m+n-2)\cdot(m+n-3) \le 0$, or $2 \le m+n \le 3$ (where $m(m-1) > 0$). □

Now we are ready to state the main result.

Theorem 2.9. *For a thin capillary meniscus with h_{xx} bounded, there can be no rupture for $n > 4$.*

Proof. Given that in Thm. 2.7 we showed that we need $m < -2$ in order to prevent rupture, and that in Thm. 2.8 we showed that we need $2 \leq m+n \leq 3$ in order for the proof of Thm. 2.7 to be valid, we can now find a bound for n above which the film cannot rupture. Since we want the smallest such bound, choose $m + n = 2$.

Then since $m + n = 2$ and $m < -2$, we can conclude that there can be no rupture in a thin capillary meniscus for $n > 4$. □

2.6 Refinement of Rupture Bounds

It is possible to refine the bound on the values of n for which rupture may occur by considering a different energy.

Theorem 2.10. *Assuming the film is symmetric, for a thin capillary meniscus with h_{xx} bounded and $\alpha < 0$, there can be no rupture for $n > 7/2$.*

Proof. Consider the energy $G = \int_\Omega h^{3/2-n}\, dx$. We wish to determine when this energy is dissipated, so we consider its time derivative. Assume symmetry of the film.

$$\begin{aligned}
\frac{\partial}{\partial t}G &= \frac{\partial}{\partial t}\int_\Omega h^{3/2-n}\, dx = \int_\Omega h_t^{3/2-n}\, dx \\
&= \left(\frac{3}{2}-n\right)\int_\Omega h^{1/2-n}h_t\, dx \\
&= \left(\frac{3}{2}-n\right)\int_\Omega h^{1/2-n}(-h^n h_{xxx})_x\, dx \\
&= \left(\frac{3}{2}-n\right)\left[-h^{1/2}h_{xxx}|_{-L}^{L} + \left(\frac{1}{2}-n\right)\int_\Omega h^{-1/2}h_x h_{xxx}\, dx\right] \\
&= \left(\frac{3}{2}-n\right)\left(\frac{1}{2}-n\right)\int_\Omega h^{-1/2}h_x h_{xxx}\, dx \\
&= \left(\frac{3}{2}-n\right)\left(\frac{1}{2}-n\right)\int_\Omega h^{-1/2}\left[\frac{\partial}{\partial x}(h_x h_{xx}) - h_{xx}^2\right]\, dx \\
&= -\left(\frac{3}{2}-n\right)\left(\frac{1}{2}-n\right)\left[\int_\Omega h^{-1/2}h_{xx}^2\, dx\left[h^{-1/2}h_x h_{xx}|_{-L}^{L}\right.\right. \\
&\quad \left.\left. + \int_\Omega \frac{1}{2}h^{-3/2}h_x^2 h_{xx}\, dx\right]\right]
\end{aligned}$$

$$= -\left(\frac{3}{2}-n\right)\left(\frac{1}{2}-n\right)\left[\int_\Omega h^{-1/2}h_{xx}^2\,dx - \frac{1}{4}\int_\Omega h^{-5/2}h_x^4\,dx \right.$$
$$\left. = -\frac{\alpha^3}{3}h^{-3/2}(L) - 2\alpha h^{-1/2}(L)h_{xx}(L)\right] \tag{2.9}$$

Now we wish to force the term in brackets to be non-negative, so that $\frac{\partial}{\partial t}G$ overall is nonpositive.

If $\alpha < 0$, then $\frac{-\alpha^3}{3}h^{-3/2}|_{-L}^{L} \geq 0$ and $-2\alpha h^{-1/2}h_{xx}|_{-L}^{L} \geq 0$ provided $h_{xx}(\pm L)$ is bounded.

Also, we can calculate

$$\left|\int_\Omega h_x^4 h^{-5/2}\,dx\right| = \left|2\int_\Omega h_x^2 h_{xx}h^{-3/2}\,dx - \frac{\alpha^3}{3}h^{-3/2}|_{-L}^{L}\right| \tag{2.10}$$

from integration by parts. Note that the second term on the right-hand side is positive.

Using the triangle inequality and the Cauchy-Schwarz inequality, we can rewrite this as

$$\left|\int_\Omega h_x^4 h^{-5/2}\,dx\right| + \frac{\alpha^3}{3}h^{-3/2}|_{-L}^{L} \leq 2\left[\int_\Omega h^{-1/2}h_{xx}^2\,dx\right]^{1/2}\left[\int_\Omega h_x^4 h^{-5/2}\,dx\right]^{1/2}, \tag{2.11}$$

which we can then square. We also divide through by the leftmost integral, since $\int_\Omega h^{-1/2}h_{xx}^2\,dx$ is one of the quantities of interest. When this is done, we are left with

$$\frac{1}{4}\int_\Omega h_x^4 h^{-5/2}\,dx + \frac{\alpha^3}{6}h^{-3/2}|_{-L}^{L} + K \leq \int_\Omega h^{-1/2}h_{xx}^2\,dx, \tag{2.12}$$

where K is a positive value encompassing the terms in the computation of the above equation which are not germane to this proof. Since K is positive, we can and will drop it from consideration without affecting the validity of the inequality.

Note that if $\alpha < 0$, we know that

$$\frac{-\alpha^3}{3}h^{-3/2}|_{-L}^{L} < \frac{-\alpha^3}{6}h^{-3/2}|_{-L}^{L}, \tag{2.13}$$

so we can write that

$$\begin{aligned}\frac{1}{4}\int_\Omega h_x^4 h^{-5/2}\,dx + \frac{\alpha^3}{3}h^{-3/2}|_{-L}^{L} &\leq \frac{1}{4}\int_\Omega h_x^4 h^{-5/2}\,dx + \frac{\alpha^3}{6}h^{-3/2}|_{-L}^{L} \\ &\leq \int_\Omega h^{-1/2}h_{xx}^2\,dx. \end{aligned}\tag{2.14}$$

And since $-2\alpha h^{-1/2} h_{xx}|_{-L}^{L} > 0$ for $\alpha < 0$, we can now look back at the bracketed term in Eqn. 2.9 and notice that Eqn. 2.14 shows that the sum of the first three terms is nonnegative, and since the last term is positive, the entire bracketed quantity is positive.

So because we can force the bracketed term to be positive, in order to dissipate the energy G we need only have

$$-\left(\frac{3}{2}-n\right)\left(\frac{1}{2}-n\right) < 0. \tag{2.15}$$

We see that the values of n that satisfy this inequality are $n > 7/2$. Since $G = \int h^{3/2-n}\, dx$, this means that if $n > 7/2$, $\int 1/h^2\, dx$ is bounded. But this integral could not be bounded if rupture occurred; therefore rupture must *not* occur for $n > 7/2$, as long as $\alpha > 0$ and h_{xx} remains bounded.

□

Unfortunately, because many of these bounding arguments rely on the sign of α being negative, this proof has not as yet been extended to the full case of no rupture for $n > 7/2$ regardless of whether $\alpha < 0$ or $\alpha > 0$.

2.7 Rupture

Beretta et al. (1995) showed that for pressure boundary conditions $h(\pm L, t) = h_{xx}(\pm L, t) = 1$, rupture will always occur in finite time for $0 < n < 1/2$. A similar result is valid for our boundary conditions, and we present the proof, with some additional physical motivation that is lacking in the proof by Beretta et al.

Theorem 2.11. *(Rupture) Let $0 < n < 1/2$, and let h_0 be a smooth positive function on $[-L, L]$ satisfying our boundary conditions, $h_x = \pm\alpha$ and $h_{xxx} = 0$ at $\pm L$. Also let h_{xx} be bounded away from zero. Then there is a time T_{h_0} such that the problem of the thin film equation with these boundary conditions and h_0 as an initial condition has a unique classical solution h satisfying $h > 0$ in $[-L, L] \times [0, T_{h_0})$ and such that the minimum value of h over the interval decreases to 0 as t approaches T_{h_0}; that is, rupture must occur.*

Proof. As many authors (e.g. Beretta et al. (1995), Bertozzi et al. (1994)) have noted, classical PDE theory allows us to claim that since $h_0(x) > 0$, there is some time t_0 for which the solution remains positive at all x, and that the solution can be continued for as long as it remains positive.

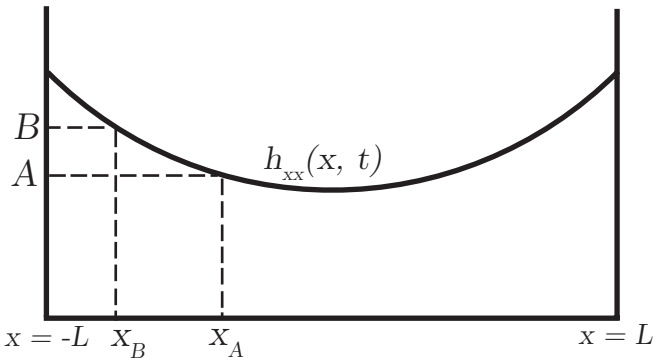

Figure 2.3: A representative plot of h_{xx}.

If we can bound h_{xx} away from zero (that is, there exists $c \in \mathbb{R}$ such that $h_{xx} \geq c > 0$), then we can find two points in the region $[-L, L]$ as shown in Fig. 2.3. Call these points x_A and x_B and let $h_{xx}(x_A) = A$ and $h_{xx}(x_B) = B$. Then, using the Cauchy-Schwarz inequality, we can compute

$$\begin{aligned} |B - A| &= |h_{xx}(x_B) - h_{xx}(x_A)| \\ &= \int_{x_A}^{x_B} h_{xxx}\, dx \\ &= \int_{x_A}^{x_B} h^{-n/2} h^{n/2} h_{xxx}\, dx \\ &= \left[\int_{x_A}^{x_B} h^{-n}\, dx\right]^{1/2} \cdot \left[\int_{x_A}^{x_B} h^n h_{xxx}^2\, dx\right]^{1/2} \end{aligned}$$

Denote the first term in brackets by P_{-n} (as in Thm. 2.8 above). Also denote the second term in brackets by D, since it describes the dissipation rate of the combined surface area/coating energy quantity which we have called E, by which we mean that a calculation can show that

$$\left|\frac{\partial E}{\partial t}\right| = \int_\Omega h^n h_{xxx}^2\, dx. \tag{2.16}$$

Then we can rearrange the above inequality to obtain

$$D \geq \frac{|B - A|^2}{P_{-n}} \geq 0. \tag{2.17}$$

We wish to bound D away from zero—that is, make the second inequality into a strict inequality—so that $E(t) \leq E(0) - Dt$, which is monotonically

decreasing for all t. This would be a contradiction, since $E(t)$ is bounded below by E_∞, the absolute energy minimizer, and this contradiction will give us the result we wish, as will become clear.

So we need to show that $|B - A|$ is bounded below and that P_{-n} is bounded above. Choose x_B and x_A such that $h_{xx}(x_B) = \max h_{xx}$ and $h_{xx}(x_A) = \min h_{xx}$, for simplicity.

Suppose that $h_{xx} > \eta$. Then $h(x) \geq \eta x^2/2$. Integrating this gives us a mass of $M \geq \eta L^3/3$, so $\eta \leq 3M/L^3$. Therefore $\min h_{xx} < 3M/L^3$.

Since $h(-L) = -\alpha$ and $h(L) = \alpha$, the Mean Value Theorem says that there is some $\xi \in [-L, L]$ such that $h_{xx}(\xi) = [\alpha - (-\alpha)]/2$. So $\max h_{xx} \geq \alpha/L$.

Using these two facts, we can state that

$$[\max h_{xx} - \min h_{xx}] \geq \left| \frac{\alpha}{L} - \frac{3M}{L^3} \right|. \tag{2.18}$$

But the mass of the film at the minimizer is $M_* = \alpha L^3/3$, so we have that

$$[\max h_{xx} - \min h_{xx}] \geq \frac{\alpha}{L} \left(1 - \frac{M}{M_*} \right), \tag{2.19}$$

which is a positive number. So $|B - A|^2$ is bounded below.

To show that P_{-n} is bounded above, consider that $h_{xx} < B$ implies that

$$h(x) \leq \frac{B(x - \bar{x})^2}{2} + C, \tag{2.20}$$

for some $\bar{x}$.

$$\frac{1}{h^n} \leq \left(\frac{2}{B} \right)^n (x - \bar{x})^{-2n}, \tag{2.21}$$

which we can integrate on both sides to find

$$\int_A^B \frac{1}{h^n}\, dx \leq \left(\frac{2}{B} \right)^n \int_{-L}^{L} \frac{1}{(x - \bar{x})^{2n}}\, dx. \tag{2.22}$$

The quantity on the right is integrable only if $2n > 1$, which implies that $n > 1/2$. So for $n > 1/2$, P_{-n} is bounded above.

We have shown that for $n > 1/2$, the dissipation rate D of the combined surface area–wetting energy term is bounded away from zero. But this is impossible—it would mean the film never achieves a minimum energy, when we know the value of the energy to be bounded below by the energy of the steady state. Our hypothesis that h_{xx} is bounded away from zero

prevents $|B - A|^2$ from *not* being bounded below, so if it is to be the case that D is *not* bounded away from zero, it must be because P_{-n} is not bounded above. But this means that P_{-n} experiences a blowup near the singularity at $\bar{x}$, which means first that the film must rupture (since this is what causes the singularity at $\bar{x}$ to be a problem) and second that we must have $n < 1/2$, since P_{-n} is integrable for $n > 1/2$.

Therefore we conclude that rupture must occur for $n < 1/2$.

□

2.8 Asymptotics

Although obtaining non-steady-state solutions to the thin film equation is generally impossible, we can make educated guesses about the behavior of the film in certain regions and obtain partial characterizations for the solutions. This is known as *asymptotics*, and generally involves postulating a particular similarity solution in a given region so that the problem is tractable to some separation of variables. Bowen and King (2001) covers this problem extensively for the case of $n < 2$, zero contact angle, and no requirement of mass conservation. Bertozzi et al. (1994) considers the problem for pressure boundary conditions, and also supports the assumptions about the nature of the asymptotics with numerical simulations.

Because of the degeneracy in the thin film equation for $h \to 0$, the boundaries of the film have a much lower relaxation time than the center of the film. This tends to create two pinch points at which the film is tending to rupture, a central "droplet" region, and the outer or "far field" regions near the boundaries. We assume that the pinch points exist at positions $x_{p,1}$ and $x_{p,2}$ which are symmetric and fixed in time. This constraint is relaxed in Bertozzi et al. (1994).

Curiously, despite the many differences between pressure and meniscus boundary conditions (most notably, pressure conditions do not require mass conservation, and certainly the contact angle is not fixed), the hypothesized asymptotic analysis is essentially the same. This is because the behavior of the central region should not be expected to change greatly from problem to problem, as its behavior is by definition largely separate from that of the far field, where the boundary conditions are applied. We might expect the behavior of the pinch region to differ, since the pinch region must be matched to the far field at the edges of the pinch, but in fact the minimizer toward which the pressure case tends is also a quadratic. So the analysis for the behavior of the pinch region is similar across both pres-

sure and meniscus boundary conditions. Our analysis in the next sections for meniscus conditions follows the one in Bertozzi et al. (1994) for pressure conditions, though in less overall detail.

2.8.1 The Central Region

If the positions of the pinch points are fixed, this fixes the length scale of the central region. It is reasonable to suppose that this allows us to consider a solution of the thin film equation as a similarity solution of the form $h(x,t) = f(t) \cdot C(x)$. If we plug this into the PDE, we get $h_t = C \cdot f_t$ and $h_{xxx} = f \cdot C_{xxx}$, which tells us that

$$C \cdot f_t + (f^{n+1} C^n C_{xxx})_x = 0, \tag{2.23}$$

which we can separate as

$$\frac{f_t}{f^{n+1}} = \frac{-(C^n C_{xxx})_x}{C} = \lambda. \tag{2.24}$$

Then we know that C solves the fourth order ODE $-(C^n C_{xxx})_x = \lambda C$ and f solves $\frac{df}{dt} = \lambda f^{n+1}$, so $f(t) = \left(\frac{1}{\lambda n t}\right)^{1/n}$.

The time dependence is what is interesting to us in situations in which there is some question of whether or not the film will ever manage to achieve its minimizer, if the progress toward that minimizer can be measured in part by the value of the central point (as it often can).

2.8.2 The Pinch Region

The pinch region's length scale may change as time increases, since fluid is flowing into and out of the region from the droplet and to the far field, respectively. Therefore we cannot separate the equation into a similarity solution in which space and time are entirely independent. Instead, as in Bertozzi et al. (1994), we consider a separation of variables $h(x,t) = \tau(t)H(\eta)$, where $\eta = (x - x_p)/\tau^q(t)$. (Bertozzi et al. (1994) do not assume that x_p is fixed with respect to time, but we continue this assumption for the sake of simplicity). This choice of similarity solution is also touched on in Myers (1998); Almgren et al. (1996).

When we substitute this similarity solution into the thin film equation, we get

$$\frac{\tau_t}{\tau}\left(1 - q\eta\frac{\partial}{\partial\eta}\right)H + \tau^{n-4q}(H^n H_{\eta\eta\eta})_\eta = 0. \tag{2.25}$$

Ordinarily there are terms describing the dependence on the time derivative of x_p, but we have assumed the pinch points are fixed, so these terms vanish. We can separate this equation into a tractable equation for τ and an intractable equation for H, as before, giving

$$\tau_t = \lambda \tau^{n-4q+1} \tag{2.26}$$

and

$$-\lambda \left(1 - q\eta \frac{\partial}{\partial \eta}\right) H = (H^n H_{\eta\eta\eta})_\eta \tag{2.27}$$

From the first of these equations we can conclude that

$$\tau(t) = \left(\frac{1}{\lambda(n-4q)t}\right)^{1/(n-4q)}. \tag{2.28}$$

We find q by matching the solution in the pinch region to the solution at the far field and center regions. In the far field, the solution converges quickly to the steady state solution, which has the form $h(x) = \alpha x^2/2L + b$. As $\eta \to \infty$, we need $H(\eta)$ to have this form, so we must have $q = 1/2$, so that the numerator of η is squared with respect to the denominator. So then we expect

$$\tau(t) = \left(\frac{1}{\lambda(n-2)t}\right)^{1/(n-2)} \tag{2.29}$$

as the time behavior of the film in the pinch region.

All of this asymptotic behavior analysis is merely hypothetical until it can be examined and compared with numerical simulations of the film's behavior. The numerical methods that would provide a mechanism for this comparison are described in the next chapter.

Chapter 3

Numerical Analysis

Since exact solutions to the thin film equation are in general difficult to find, except in a few restrictive situations such as the steady-state solution above the critical mass, we chose to also approach the problem from a numerical standpoint.

3.1 Implementation

3.1.1 Overall Behavior

Though we used two different implementations to solve the numerical problem itself, discussed below in Sec. 3.1.2, the generic code that wraps the solver can be essentially the same for any implementation. The main MATLAB routine accepts from the user a number of inputs, namely:

- the exponent n in the thin film equation;
- the contact angle α at the right-hand boundary;
- the number of gridpoints desired;
- a vector of length (gridpoints + 1), describing the initial condition;
- the total time T for which to run the solver;
- and in the case of one method, a solution parameter θ whose purpose is described in Sec. 3.1.4.

It is worth noting that one primary difference between all our theoretical analysis and this numerical code is that the theoretical analysis has all

been done on the interval $[-L, L]$, whereas all numerical computation is normalized to the interval $[0, 1]$.

In addition to the main solver and the routines it calls, there are a number of associated helper routines, such as a function which can generate the minimum plots described in Sec. 3.3, and a function which will play back an animation of the evolution of the film as time progresses.

3.1.2 Methods of Solving Large Nonlinear Systems of ODEs

In order to solve the thin film equation numerically, we first discretize it along the spatial variable x into a system of coupled nonlinear fourth-order ODEs. Our implementation uses a static mesh (the gridpoints are fixed in location and number) because it is computationally cheaper, but because the equation $h_t + (h^n h_{xxx})_x = 0$ becomes degenerate as $h \to 0$, it is common to use a dynamically adaptive mesh (one such that gridpoints can be added, subtracted, or moved) that can be refined near pinch points in order to avoid instabilities in the simulation.

If we define the N equally spaced mesh points to be $x_0, x_1, \ldots, x_N$, it is customary in the literature to use y_i to denote the numerical approximation to the exact value $h(x_i)$. We will follow this convention throughout this section.

To define the discretized ODEs, we use finite difference methods. This scheme is described extensively in Bertozzi (1998). Following that paper's notation, we denote the finite differences by

$$\begin{aligned} y_{\bar{x},i} &= \frac{y_i - y_{i-1}}{\Delta x} \\ y_{\bar{x}x,i} &= \frac{y_{\bar{x},i+1} - y_{\bar{x},i}}{\Delta x} \\ y_{\bar{x}x\bar{x},i} &= \frac{y_{\bar{x}x,i} - y_{\bar{x}x,i-1}}{\Delta x}, \end{aligned} \tag{3.1}$$

where an $\bar{x}$ denotes a backward difference and an x denotes a forward difference.

We also define a function $a(y_i, y_j)$ by

$$a(y_i, y_j) = \begin{cases} \frac{y_i - y_j}{G'(y_i) - G'(y_j)} & \text{if } y_i \neq y_j, \\ y_i^n & \text{if } y_i = y_j, \end{cases} \tag{3.2}$$

where $G(y_i)$ is a function satisfying $G''(y_i) = 1/y_i^n$. For our purposes, it is sufficient to integrate G'' up once and ignore the constant of integration.

The finite differences and the function $a(y_i, y_j)$ allow us to write the coupled system of ODEs as

$$(y_i)_t + (a(y_{i-1}, y_i)y_{\bar{x}xx,i})_x = 0, \tag{3.3}$$

where again the x at the end of the parentheses denotes a forward difference.

It is shown in Zhornitskaya and Bertozzi (2000) that for the choice of $a(y_i, y_j)$ in Eqn. 3.2, this numerical scheme is positivity-preserving.

Once this discretization is complete, the next step is to solve the system of ODEs it creates. At this point, there is a plethora of options. Over the course of this thesis, we have used two separate methods: first a built-in MATLAB solver, and later a from-scratch method using θ-weighted schemes and Newton-Raphson iteration.

One factor that must be taken into account when choosing a scheme for solving the system of ODEs is that the thin film equation becomes degenerate as the film tends toward rupture. We are therefore dealing with a *stiff problem*, that is, a simulation for which we must choose a highly refined timestep in order to maintain stability of the solution scheme.

3.1.3 Method One: Built-In Routine

MATLAB has a number of built-in ODE solving routines, each of which has its own separate strengths and weaknesses. We chose to use `ode15s`, which is a solver intended for stiff problems when typical Runge-Kutta/Dormand-Prince methods fail or are too slow.

Advantages

- Employs dynamic timesteps and can therefore reduce its step size to maintain accuracy only when the problem's stiffness begins to come into play, allowing a coarse timestep and computational efficiency when the system of ODEs is not degenerate and the problem is not stiff.
- This solution scheme is robust to choices of initial condition that do not match the boundary conditions exactly, allowing vast freedom in the choice of initial condition. When a poor choice of initial condition is given, the code corrects within one timestep to a solution which does satisfy the boundary conditions.

Disadvantages

- The code cannot continue solving when the solution becomes negative, but it has no way to stop solving before the time specified by the user. Instead it continues to refine its timestep endlessly near the time at which rupture occurs, attempting to find a timestep fine enough to accommodate the degeneracy (which it cannot do). This makes it unwise to leave a long job running unattended, since the code may get stuck and be unable to extricate itself.
- The code intermittently responds poorly to attempts to force it to quit using Ctrl-C, and may cause a segmentation fault.
- The scheme is essentially a "black box." The documentation files are sparse regarding the actual algorithm, and the code for the scheme itself is arcane and not heavily commented, making it difficult to determine which method it is actually using.

3.1.4 Method Two: θ-Weighted Schemes

Let y_i denote the value of the film height at the ith gridpoint. Because there are four spatial derivatives in the original thin film equation, the successive finite differences we take to approximate these derivatives cause us to lose the ability to define the ODEs on the two boundary points at each end (a total of four). Fortunately, we also have four boundary conditions: $h_x(\pm L) = \alpha$ and $h_{xxx}(\pm L) = 0$. By forcing the film height at any given timestep to satisfy these boundary conditions, we can get the four additional constraints

$$y_1 - \frac{12}{5}y_3 + \frac{64}{35}y_4 - \frac{3}{7}y_5 = \frac{36}{35}\alpha\Delta x,$$

$$y_2 - 2y_3 + \frac{9}{7}y_4 - \frac{2}{7}y_5 = \frac{2}{7}\alpha\Delta x,$$

$$y_n - 2y_{n-1} + \frac{9}{7}y_{n-2} - \frac{2}{7}y_{n-3} = \frac{2}{7}\alpha\Delta x,$$

and

$$y_{n+1} - \frac{12}{5}y_{n-1} + \frac{64}{35}y_{n-2} - \frac{3}{7}y_{n-3} = \frac{36}{35}\alpha\Delta x,$$

using tedious algebra which I will not reproduce here.

Each time ODE is given by the equation

$$\frac{\partial y_i}{\partial t} + \frac{1}{\Delta x}\left[a(y_i, y_{i+1})y_{\bar{x}x\bar{x},i+1} - a(y_{i-1}, y_i)y_{\bar{x}x\bar{x},i}\right] = 0,$$

where

$$y_{\bar{x}x\bar{x},i} = \frac{y_{i+1} - 3y_i + 3y_{i-1} - y_{i-2}}{\Delta x^3}.$$

Call each of these equations F_i. Because of the multiple finite difference equations that must be evaluated to construct each F_i, it is impossible to construct F_i for the two points on each end of the solution interval. We can define these F_i for all other gridpoints. Now we have $n+1$ equations ($n-3$ from the interior points, and 4 more from boundary condition matching) and $n+1$ unknowns, the value at any given time of y_i for each mesh point.

The derivation of the values used in the Newton-Raphson method begins with θ-weighted schemes. In such a scheme, we say that

$$\frac{y_{n,i} - y_{o,i}}{\Delta t} = \theta F_i(y_n) + (1-\theta)F_i(y_o),$$

where $y_{o,i}$ is the value of the film at the ith gridpoint before the timestep, $y_{n,i}$ is the value at the ith gridpoint after the timestep, and F_i is the operator determined by the thin film equation acting on the vector of film heights, y_n or y_o.

Rearranging this, we can write

$$y_{n,i} - \Delta t(1-\theta)F_i(y_n) = y_{o,i} + \Delta t\theta F_i(y_o).$$

Call the left-hand side of this equation $N(y_n)$ and the right-hand side $R(y_o)$. Then include the four additional constraint equations, with all terms involving a y_i on the left-hand side and all the constant terms involving α and Δx on the right-hand side. Let the collection of $N(y_n)$ and the left-hand side of the constraints be denoted $\mathfrak{N}(y_n)$, and let the collection of $R(y_n)$ and the right-hand side of the constraints be called $\mathfrak{R}(y_o)$. Together, these things imply that $\mathfrak{N}(y_n) = \mathfrak{R}(y_o)$.

In order to use the Newton-Raphson method in MATLAB, taking advantage of MATLAB's powerful matrix inversion tools, we need to linearize this system. First, use Taylor expansion on $\mathfrak{N}(y_n)$ to get

$$\mathfrak{N}(y_n) = \mathfrak{N}(y_o) + \mathfrak{J}(y_o)\cdot\delta y,$$

where $\mathfrak{J}$ is the Jacobian matrix of the operator $\mathfrak{N}$. Now, using the fact that $\mathfrak{N}(y_n) = \mathfrak{R}(y_o)$, we can write

$$\mathfrak{R}(y_o) = \mathfrak{N}(y_o) + \mathfrak{J}(y_o)\cdot\delta y,$$

which rearranges to

$$\delta y = \mathfrak{J}^{-1}(y_o)\left[\mathfrak{R}(y_o) - \mathfrak{N}(y_o)\right].$$

Because of the form of the functions F_i and of the boundary constraints, $\mathfrak{J}$ is a band matrix of band width 5, since the entries in the Jacobian are $\partial F_i/\partial y_j$, and F_i depends only on y_j for $j = i-2, i-1, i, i+1$, and $i+2$. So if the number of gridpoints is large enough, $\mathfrak{J}$ is also extremely sparse.

Once we get δy from this computation, we can add it to y_o and either iterate this process some number of times before we return y_n, or return $y_n = y_o + \delta y$ right away and proceed another timestep. A quick method of checking whether the code is functioning properly is that for the linear case, when $n = 0$, the Newton-Raphson iteration should converge in a single step, so it should not be necessary to iterate more than once during any given timestep.

Advantages

- The scheme itself is quite simple. None of the mathematics in the above derivation need take place in the program itself, so the only computation involves creation and inversion of the Jacobian, and multiplication of this inverse by a vector. The Jacobian is an extremely sparse band matrix of band width 5, so the inversion is relatively computationally cheap.
- The code allows the user to specify a fully implicit scheme, a fully explicit scheme, or an intermediate mixed scheme. This allows the user to make a tradeoff between speed and stability.
- There is a catch in the code that allows the simulation to stop if the film height ever becomes negative, preventing the code from running for unnecessarily long times.

Disadvantages

- Unlike `ode15s`, this scheme is not at all robust to poor choices of initial condition. It quickly becomes unstable and often experiences blowup at the boundary.
- Despite the current lack of dynamic timestep, this scheme takes longer to run than methods using `ode15s`.

- Where `ode15s` may respond poorly to Ctrl-C, this method occasionally seemingly fails to respond at all. This may simply be the result of high computational requirements causing a lag in response time.

3.2 Observation of Film Behavior

3.2.1 Rupture and Critical Exponents

Though it has been shown that $n \geq 7/2$ is sufficient to preclude rupture in a film with periodic boundary conditions, and we have shown that $n > 4$ is sufficient for a thin capillary meniscus, it is hypothesized that the actual bound is much lower, and that in fact there may be some critical exponent n_*, possibly dependent on boundary conditions, above which we can definitively state that rupture cannot occur and below which we admit the possibility that rupture may occur. Currently we can guarantee for certain boundary conditions that rupture can occur for $n < 1/2$, but cannot make definitive assertions about $1/2 < n < 7/2$.

Making theoretical progress on this problem is hard, but we can make some numerical observations which seem to bear out this possibility. Consider, for instance, Figure 3.1, in which for $n = 1$ we set the initial condition of the film to be $(.5 - x)^2 + .05e^{-10x^2}$ and allowed the ODE solver to run until the film ruptured. At $t = .00675$, we can see from the figure that the film touches down; after this point the solver cannot continue running because the film height would become negative.

Now compare Figure 3.1 to Figure 3.2, which is of a film with the same initial conditions, but with $n = 2$ and the simulation carried out until $t = .15$. The film in Figure 3.2 has not ruptured (though we can see that it is becoming quite thin) despite having been run all the way until $t = .15$, whereas the first film ruptured after only $t = .00675$. Not only that, but this film is beginning to form a droplet in the center, between a pair of points at which the film height is approaching 0, though it has not reached it.

As we refine the number of gridpoints on which the PDE is being solved, these "squeezing points" may shift position in the interval; certainly their positions shift over time. We can have the MATLAB routine save the data from its simulation and use these data to determine how and how fast these points are shifting, though we have not done any of this yet.

For additional comparison between the rupture and squeeze points for $n = 1$ and $n = 2$, consider the following pair of figures, Figs. 3.3 and 3.4, which zoom in on the right-hand rupture and squeeze points from Figs. 3.1

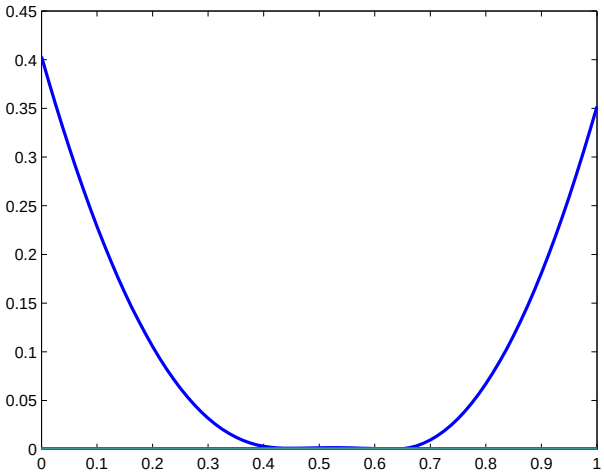

Figure 3.1: A ruptured film with $n = 1$ and $t = .00675$.

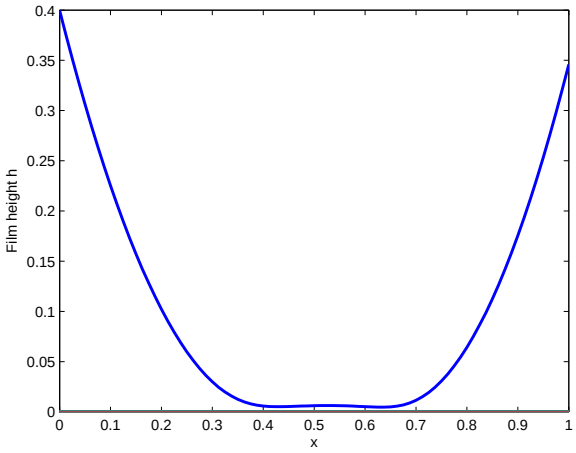

Figure 3.2: A small droplet forming in a film for $n = 2$, $t = .15$.

and 3.2. Note the actual touchdown point in the $n = 1$ case, whereas in the $n = 2$ case a significant film thickness remains.

This comparison of Figs. 3.1 and 3.2 is only one example of many such

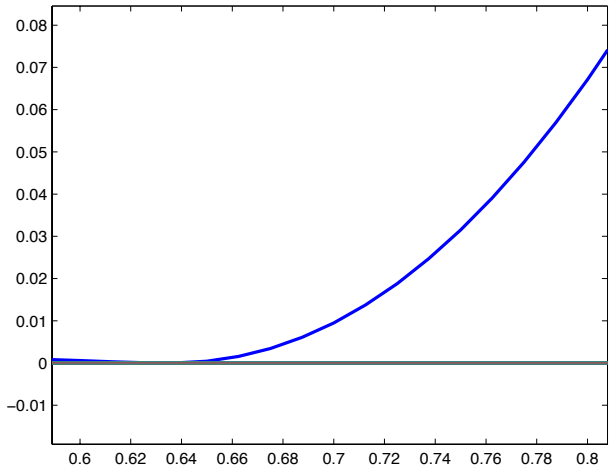

Figure 3.3: A close-up of the rupture in Fig. 3.1 for $n = 1$, $t = .00675$.

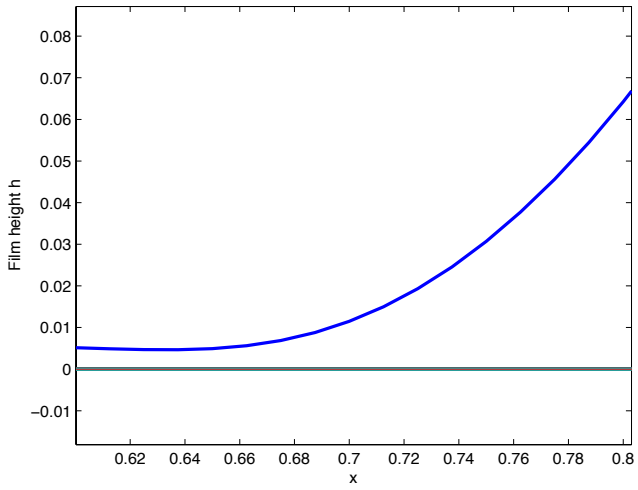

Figure 3.4: A close-up of a squeeze point in Fig. 3.2 for $n = 2$, $t = .15$.

pairs of figures in which the film is below the critical mass for $n = 1$ and therefore ruptures, yet does not seem to do so in finite time for $n = 2$. It

may rupture in infinite time, or it may not rupture at all; it requires further simulation and data analysis to more firmly hypothesize which.

3.2.2 Minimizers

Clearly we would like to know that our theoretical results and the numerical simulations are in agreement. In particular, we would like to know that the numerical code demonstrates that films do in fact approach the quadratic minimizer we gave for the energy E in Sec. 2.2.3.

In practice, however, it is not always obvious that this is the case. Certainly particular initial conditions cause the film to converge quickly to the minimizer, as in Figure 3.5, which had an initial condition of simply the constant .5 across the entire interval and converged to the quadratic minimizer by $t = .05$.

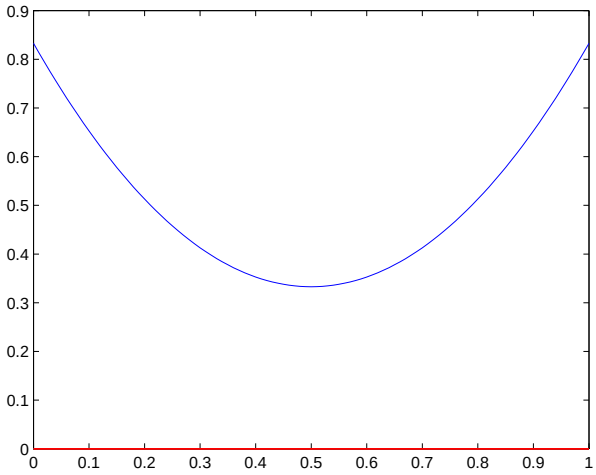

Figure 3.5: Convergence to a minimizer for $n = 2$, $t = .05$.

In other cases, however, such as Figure 3.2 above, rather than achieving the minimizer, the film forms a droplet between two points whose thickness is squeezed as time passes. (In fact, the beginnings of this droplet behavior are often visible in animations of films that *do* achieve their minimizers, but usually the droplet quickly smooths out.) This droplet is not piecewise quadratic, and we would like to know whether the film ever re-

laxes into a quadratic as current theory suggests it should.

If in fact numerical results continue to suggest that some films do not approach a quadratic minimizer in finite or infinite time, our next goal would be to attempt to prove theoretically that this is can be the case or perhaps find another energy whose minimizers more accurately describe those observed numerically.

3.3 Refinement Analysis

With the data our solver outputs, we can generate a plot of the minimum thickness of the film (on a logarithmic scale) against the time t at which these minima occurred. The goal is to use an analysis of these plots of the minima to determine whether or not the film will rupture in finite time, infinite time, or not at all.

The specific method of refinement studies we will use is to halve or double the coarseness of the solution mesh, draw two `minplots` on top of one another, and observe the differences in scaling of film thickness with the coarseness of the mesh.

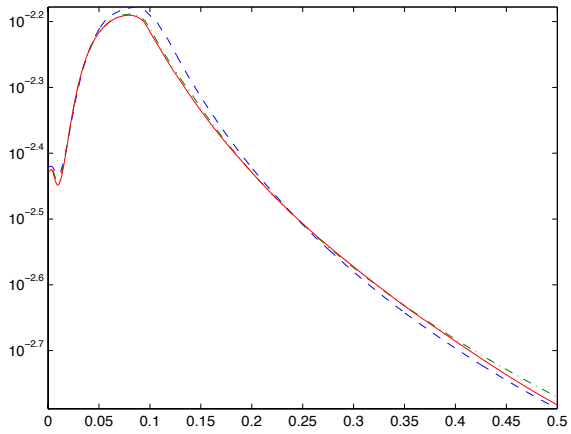

Figure 3.6: Minimum thickness of the film over time.

As an illustration, consider Figure 3.6, which shows the minimum plots for the same film for which a time snapshot is given in Figure 3.2. The minimum plots are given for 40, 80, and 160 gridpoints; the solid line is for

40, the dashed line for 80, and the dotted and dashed line for 160. We can already see that the numerical solution is converging fairly well, as these plots lie nearly on top of one another much of the time.

We can also plot the absolute value of the difference between two arrays of values for minimum film thickness over time, usually using the most refined values as a baseline and subtracting the others from these. We could use these plots to see how the error between a well-refined film and an under-refined film is scaling, e.g. proportionally, as the square, and so forth. Figure 3.7 is an example of this type of plot, in which we can see that doubling the number of gridpoints seems to decrease the error in the minimum values of the film by approximately one order of magnitude. In that figure, the solid line is the baseline minimum film thickness for 160 gridpoints, with the difference between 160 and 40 gridpoints being shown as a dashed line and the difference between 160 and 80 gridpoints shown as a dotted and dashed line. The main goal of refinement analysis is to show that the numerical code actually converges to a single solution if the number of gridlines is sufficiently high. From Figs. 3.6 and 3.7, we can see that even at only 160 gridpoints, the code is already converging fairly quickly.

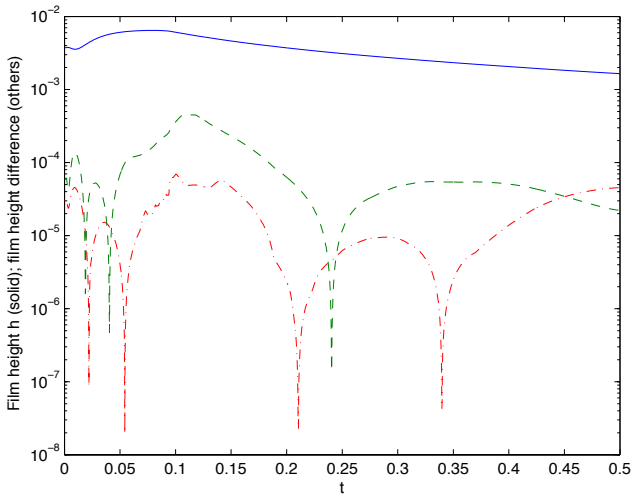

Figure 3.7: Refinement analysis plot for `ode15s` solver.

In addition to the figures, whose only purpose is to give us a quick visual summary of the behavior of the minimum values, we also save the

data which generated these minimum plots so that we can analyze it later.

We can also attempt to track the *location* of these minima. In general, it seems to be the case that the film will do one of the following things:

- Converge to a minimizer without rupture,
- Experience a single touchdown or squeeze point, or
- Experience a pair of touchdown or squeeze points.

In the last case, we wish to observe the change in position of the pinch points, hoping to determine whether they will move inward and merge together, whether they will stay in one location and simply squeeze progressively thinner, or whether they will disappear and the film will converge to the quadratic minimizer. This is a matter for further investigation. It is also not clear whether it is possible to force the film to experience more than two touchdown points, but so far the numerical simulations generated for this thesis have been unable to do so.

Chapter 4

Future Work

We have reproduced many of the familiar rupture and no-rupture results from studies on other boundary conditions and stated some results concerning the behavior of the film in a steady state. The study of the thin film equation, however, still offers a wealth of deep problems for investigation.

4.1 General Open Problems

For the thin film equation in general, with no specific choice of boundary condition, by far the largest open problem is the critical exponent problem. Does there exist an exponent n_* above which rupture cannot occur and below which rupture must occur? If so, is its exact value dependent on the choice of boundary conditions? Does it exist for certain boundary conditions but not for others? Currently the best bounds which have no additional restrictions are that rupture must occur in finite time for $n < 1/2$ and cannot occur for $n > 7/2$, for periodic boundary conditions.

The general consensus in the research community (see for instance the discussion in Bertozzi (1998)) seems to be that such a sharp bound between rupture and no rupture does in fact exist and that $n_* = 2$, but there exists no proof of this fact for any boundary conditions. Bertozzi et al. (1994) have managed to refine the no-rupture bound to $n \geq 2$ for pressure boundary conditions, but only provided that h_{xx} is bounded, which it is not easy to guarantee. Interestingly, it can be proven that certain numerical schemes cannot rupture for $n \geq 2$ (see Zhornitskaya and Bertozzi (2000)), but the same proof cannot be extended to the theoretical problems these schemes model.

4.2 Problems Specific to the Capillary Meniscus

4.2.1 Theoretical Problems

Many of the proofs in this paper still have the frustrating restriction that they must assume that h_{xx} is bounded. It would be desirable to remove this restriction, either by proving that h_{xx} is always bounded in the relevant cases, or by finding alternate proofs that avoid needing to bound h_{xx}.

Moreover, currently we can only refine the no-rupture bound to exponents $n \geq 7/2$ for films with $\alpha < 0$, that is, films which do not wet the walls. Physical intuition suggests that we would not expect such films to rupture in any case (drying up in the middle only forces them to coat the walls more), so we would like to extend this proof to films with $\alpha > 0$ to obtain the full result of no rupture for $n \geq 7/2$.

Finally, because of the degeneracy in the problem as $h^n \to 0$, the time required for the film to relax to a steady state at the boundary (far field) is much smaller than the time required for the central and pinch regions to relax. This is what causes the droplet formation in the central region. For films below the critical mass, but for an exponent for which rupture cannot occur, we would like to know if these films ever converge to a quadratic minimizer or if instead communication between the central region and the far field is cut off by the degeneracy in the pinch region. If the latter case is true, we wish to find new energies which explain this behavior, and moreover we wish to determine the steady-state behavior of the film.

4.2.2 Numerical Problems

We have illustrated only preliminary work in the numerics of this problem, and there is much still to be done. Certainly each variation of the numerical code could benefit from the correction of their primary disadvantages so that they are actually useful for solving numerical problems.

The most interesting open numerical problem for the capillary meniscus is the question of whether the similarity solutions of the form theorized in Sec. 2.8 are in fact borne out by numerical simulations. The time behavior of the central and pinch regions is relatively easy to check; it is a simple operation in MATLAB to pull out the central or minimal element of the height vector at each timestep, and these points can then be transferred to a data analysis package such as `gnuplot` to be curve fit. Similar methods could be used to answer the question above in the theory section about the behavior of films below the critical mass but above the no-rupture bound

on the exponent. The computational investment in either case, however, is significant, and we recommend the use of at least one computer which is dedicated to the task and need not share its processing power.

Bibliography

Robert Almgren. Singularity formation in Hele-Shaw bubbles. *Phys. Fluids*, 8(2):344–352, 1996.

Robert Almgren, Andrea Bertozzi, and Michael P. Brenner. Stable and unstable singularities in the unforced Hele-Shaw cell. *Phys. Fluids*, 8(6): 1356–1370, 1996.

Elena Beretta, Michiel Bertsch, and Roberta Dal Passo. Nonnegative solutions of a fourth-order nonlinear degenerate parabolic equation. *Arch. Ration. Mech. Anal.*, 129(2):175–200, 1995.

Francisco Bernis and Avner Friedman. Higher order nonlinear degenerate parabolic equations. *J. Differential Equations*, 83:179–206, 1990.

A. J. Bernoff and T. P. Witelski. Linear stability of source-type similarity solutions of the thin film equation. *Appl. Math. Lett.*, 15(5):599–606, 2002. ISSN 0893-9659.

A. L. Bertozzi. Symmetric singularity formation in lubrication-type equations for interface motion. *SIAM J. Appl. Math.*, 56:681–714, 1996.

A.L. Bertozzi. Loss and gain of regularity in a lubrication equation for thin viscous films. In *Proceedings of the International Colloquium on Free Boundary Problems*, Toledo, Spain, 1993.

A.L. Bertozzi and M. Pugh. The lubrication approximation for thin viscous films: Regularity and long-time behavior of weak solutions. *Comm. Pure Appl. Math.*, 49:85–123, 1996.

Andrea L. Bertozzi. The mathematics of moving contact lines in thin liquid films. *Notices Amer. Math. Soc.*, 45(6):689–697, 1998. ISSN 0002-9920.

Andrea L. Bertozzi, Michael P. Brenner, Todd F. Dupont, and Leo P. Kadanoff. Singularities and similarities in interface flows. In *Trends and perspectives in applied mathematics*, volume 100 of *Appl. Math. Sci.*, pages 155–208. Springer, New York, 1994.

M. Bowen and J.R. King. Asymptotic behavior of the thin film equation in bounded domains. *European J. Appl. Math.*, 2(3):321–356, 2001.

J. A. Carrillo and G. Toscani. Long-time asymptotics for strong solutions of the thin film equation. *Comm. Math. Phys.*, 225(3):551–571, 2002. ISSN 0010-3616.

Peter Constantin, Todd F. Dupont, Raymond E. Goldstein, Leo P. Kadanoff, Michael J. Shelley, and Su-Min Zhou. Droplet breakup in a model of the Hele-Shaw cell. *Phys. Rev. E*, 47(6):4169–4181, 1993.

Stephen H. Davis. Interfacial fluid dynamics. In G.K. Batchelor, H.K. Moffatt, and M.G. Worster, editors, *Perspectives in Fluid Dynamics*, chapter 1, pages 1–51. Cambridge University Press, 2002.

Todd F. Dupont, Raymond E. Goldstein, Leo P. Kadanoff, and Su-Min Zhou. Finite-time singularity formation in Hele-Shaw systems. *Phys. Rev. E*, 47(6):4182–4196, 1993.

J. R. King. Exact multidimensional solutions to some nonlinear diffusion equations. *Quart. J. Mech. Appl. Math.*, 46(3):419–436, 1993. ISSN 0033-5614.

R. S. Laugesen. New dissipated energies for the thin fluid film equation. *Commun. Pure Appl. Anal.*, X(X):33, 2004.

R.S. Laugesen and M.C. Pugh. Linear stability of steady states for thin film and Cahn-Hilliard type equations. *Arch. Ration. Mech. Anal.*, 154(1):3–51, 2000.

T.G. Myers. Thin films with high surface tension. *SIAM Review*, 40(3):441–462, 1998.

H. Ockendon and J.R. Ockendon. *Viscous Flow*. Cambridge University Press, 1995.

Alexander Oron, Stephen H. Davis, and S. George Bankoff. Long-scale evolution of thin liquid films. *Rev. Mod. Phys.*, 69(3):931–980, 1997.

L. Zhornitskaya and A. L. Bertozzi. Positivity-preserving numerical schemes for lubrication-type equations. *SIAM J. Numer. Anal.*, 37:523–555, 2000.